Inorganic Chemistry

Article

pubs.acs.org/IC

Synthesis, Structures, and Dearomatization by Deprotonation of Iron Complexes Featuring Bipyridine-based PNN Pincer Ligands

Thomas Zell,[†] Robert Langer,[†] Mark A. Iron,[‡] Leonid Konstantinovski,[‡] Linda J. W. Shimon,[‡] Yael Diskin-Posner,[‡] Gregory Leitus,[‡] Ekambaram Balaraman,[†] Yehoshoa Ben-David,[†] and David Milstein*[,†]

[†]Department of Organic Chemistry and [‡]Department of Chemical Research Support, Weizmann Institute of Science, 76100 Rehovot, Israel

Supporting Information

ABSTRACT: The synthesis and characterization of new iron pincer complexes bearing bipyridine-based PNN ligands is reported. Three phosphine-substituted pincer ligands, namely, the known ^{t}Bu-PNN (6-((di-*tert*-butylphosphino)methyl)-2,2′-bipyridine) and the two new ^{i}Pr-PNN (6-((di-*iso*-propylphosphino)methyl)-2,2′-bipyridine) and Ph-PNN (6-((diphenylphosphino)methyl)-2,2′-bipyridine) ligands were synthesized and studied in ligation reactions with iron(II) chloride and bromide. These reactions lead to the formation of two types of complexes: *mono*-chelated neutral complexes of the type [(R-PNN)Fe(X)$_2$] and *bis*-chelated dicationic complexes of the type [(R-PNN)$_2$Fe]$^{2+}$. The complexes [(R-PNN)Fe(X)$_2$] (**1**: R = ^{t}Bu, X = Cl, **2**: R = ^{t}Bu, X = Br, **3**: R = ^{i}Pr, X = Cl, and **4**: R = ^{i}Pr, X = Br) are readily prepared from reactions of FeX$_2$ with the free R-PNN ligand in a 1:1 ratio. Magnetic susceptibility measurements show that these complexes have a high-spin ground state (S = 2) at room temperature. Employing a 2-fold or higher excess of ^{i}Pr-PNN, diamagnetic hexacoordinated dicationic complexes of the type [(^{i}Pr-PNN)$_2$Fe](X)$_2$ (**5**: X = Cl, and **6**: X = Br) are formed. The reactions of Ph-PNN with FeX$_2$ in a 1:1 ratio lead to similar complexes of the type [(Ph-PNN)$_2$Fe](FeX$_4$) (**7**: X = Cl, and **8**: X = Br). Single crystal X-ray studies of **1**, **2**, **4**, **6**, and **8** do not indicate electron transfer from the Fe^{II} centers to the neutral bipyridine unit based on the determined bond lengths. Density functional theory (DFT) calculations were performed to compare the relative energies of the *mono*- and *bis*-chelated complexes. The doubly deprotonated complexes [(R-PNN*)$_2$Fe] (**9**: R = ^{i}Pr, and **10**: R = Ph) were synthesized by reactions of the dicationic complexes **6** and **8** with KO^{t}Bu. The dearomatized nature of the central pyridine of the pincer ligand was established by X-ray diffraction analysis of single crystals of **10**. Reactivity studies show that **9** and **10** have a slightly different behavior in protonation reactions.

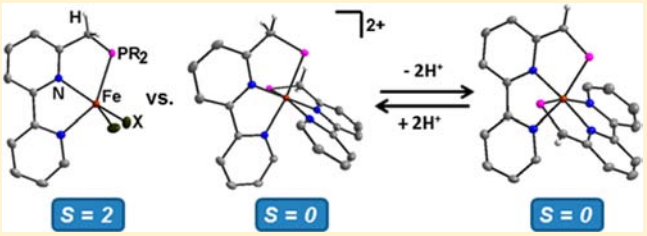

INTRODUCTION

Iron pincer complexes have attracted much interest in recent years. Since the initial reports on the application of *bis*(imino)-pyridine iron complexes as catalysts in olefin oligomerization and polymerization reactions by Brookhart[1] and Gibson[2] in the late 1990s, iron pincer complexes have been extensively studied in these reactions.[3] Chirik and co-workers later showed that *bis*(imino)pyridine-iron complexes are efficient catalysts for various reactions such as hydrogenation of olefins and alkynes,[4] and hydrosilylation of olefins, alkynes, aldehydes, and ketones.[4a,5]

Besides the use of iron pincer complexes as homogeneous catalysts for various types of reactions,[3h] this class of complexes was used for the specific binding[6] and stoichiometric activation of substrates,[7] and it has been discussed in the context of molecular sensors and switches.[8]

Our group recently reported the synthesis of the PNP-based iron pincer complex [(^{i}Pr-PNP)Fe(H)(CO)(Br)][9] (**A**, Scheme 1, ^{i}Pr-PNP = 2,6-bis(di-*iso*-propylphosphinomethyl)pyridine) and the related [(^{i}Pr-PNP)Fe(H)(CO)(η-BH$_4$)][10] (**B**, Scheme 1), which are efficient catalysts for the hydrogenation of ketones under mild conditions. Furthermore, we found that the pincer complex [(^{t}Bu-PNP)Fe(H)$_2$(CO)] (**C**, Scheme 1, ^{t}Bu-PNP = 2,6-bis(di-*tert*-butylphosphinomethyl)pyridine) is an efficient catalyst for the hydrogenation of carbon dioxide to sodium formate in aqueous sodium hydroxide solutions at remarkably low pressures and temperatures.[11] Further investigations on the application of this complex as catalyst for the formal reverse reaction revealed a very high activity in the decomposition of formic acid to CO$_2$ and H$_2$ in the presence of trialkylamines.[12]

Over the past few years, we have explored the dearomatized, bipyridine-based pincer complex [(^{t}Bu-PNN*)Ru(H)(CO)] (**D**, ^{t}Bu-PNN = 6-(di-*tert*-butylphosphinomethyl)-2,2′-bipyridine Scheme 1, the asterisk denotes a dearomatized pincer ligand) as a catalyst for various environmentally benign catalytic processes. **D** has been used as a catalyst for the hydrogenation of amides to the corresponding alcohols and amines,[13] the hydrogenation of urea derivatives to amines and methanol,[14] the hydrogenation of organic carbonates, carbamates, and

Received: June 6, 2013
Published: July 31, 2013

dx.doi.org/10.1021/ic401432m | Inorg. Chem. 2013, 52, 9636−9649

Scheme 1. Iron and Ruthenium Pincer Complexes A–D

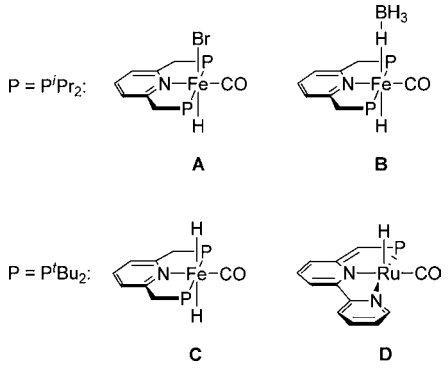

formates to the corresponding alcohols and amines,[15] and the hydrogenation of cyclic diesters to afford 1,2-diols.[16] Furthermore, coupling of nitriles with amines to form imines,[17] the cross-esterification reaction of primary alcohols with secondary alcohols,[18] and the transformation of alcohols to carboxylic acids and dihydrogen using water as an oxygen source are catalyzed by **D**.[19] Very recently the direct synthesis of pyrroles via dehydrogenative coupling of β-aminoalcohols with secondary alcohols,[20] as well as selective deuteration reactions of alcohols employing D_2O as deuterium source[21] catalyzed by **D** were reported.

The extraordinary activity of the bipyridine-based ruthenium pincer complex **D** prompted us to investigate the synthesis and the properties of the corresponding iron complexes. Herein we report on the ligation of the P-substituted bipyridine-based PNN ligands (^{t}Bu-PNN = 6-((di-*tert*-butylphosphino)methyl)-2,2′-bipyridine, ^{i}Pr-PNN = 6-((di-*iso*-propylphosphino)methyl)-2,2′-bipyridine, and Ph-PNN = 6-((diphenylphosphino)methyl)-2,2′-bipyridine; Scheme 2) with iron(II) chloride and bromide. During the finalization of our manuscript, a report on the application of complex **1** (Scheme 3) as precatalyst for the hydroboration of alkenes with pinacolborane was published by Huang and co-workers.[22]

Scheme 2. Ligands Used in This Paper

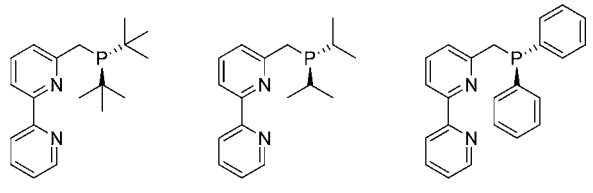

Scheme 3. Synthesis of Complexes 1 and 2

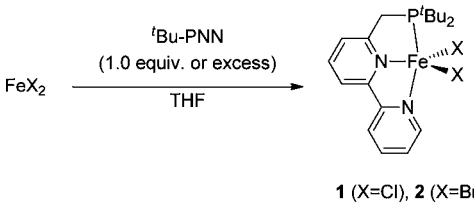

RESULTS AND DISCUSSION

The reactions of ^{t}Bu-PNN with $FeCl_2$ or $FeBr_2$ in tetrahydrofuran (THF) lead to formation of the dihalide complexes [(^{t}Bu-PNN)Fe(Cl)$_2$] (**1**) and [(^{t}Bu-PNN)Fe(Br)$_2$] (**2**) as red and black complexes, respectively (Scheme 3). Elemental analyses of the compounds are in good agreement with the expected formulation, and the electrospray ionization-mass spectrometry (ESI-MS) spectra show characteristic ions, such as the corresponding complex cations [(^{t}Bu-PNN)Fe(X)]$^+$.

The ^{1}H NMR spectra of both compounds show nine paramagnetically shifted resonances, which are tentatively assigned to the seven resonances of the bipyridyl unit, one resonance for the CH_2 group, and one resonance for the methyl protons of the ^{t}Bu groups. This pattern indicates a plane of symmetry through the iron pincer moiety in solution. The signals appear in the range of −15.76 to 128.43 ppm and −13.02 to 116.50 ppm for complexes **1** and **2**, respectively. In the ^{31}P{^{1}H} NMR spectra, no resonances are observed for these compounds in the range of −4000 to +4000 ppm. Magnetic measurements in solution at room temperature (Evans' method[23]) gave effective magnetic moments of μ_{eff} = 5.0 (for complex **1**) and 5.3 μ_B (for complex **2**), which are consistent with S = 2 spin ground states.

X-ray diffraction analyses clearly confirm the formation of the dihalide complexes **1** and **2** (see Figure 1). The molecular structures of both complexes in the solid state are best described as strongly distorted trigonal bipyramidal coordination of the iron atoms, with N1 and P occupying the apical positions. Other structurally characterized pincer complexes of the type [(PNN)-Fe(X)$_2$] exhibit similar structures.[24] The N1–Fe–P angles of 151.37(5)° (for **1**) and 148.57(4)° (for **2**) strongly deviate from the ideal linear geometry. The CH_2P arm is bent out of the plane of the bipyridine–iron unit (N1, N2, Fe): the distances of the P atoms to this plane are 0.6388(6) and 0.5974(4) Å for complexes **1** and **2**, respectively. The Fe–P bond distance of complex **1** (2.5574(7) Å) is somewhat longer than in the case of complex **2** (2.5034(5) Å).

As in the cases of ^{t}Bu-PNN, the complexes [(^{i}Pr-PNN)Fe-(X)$_2$] (X = Cl **3** and X = Br **4**, Scheme 4) are obtained by the reactions of ^{i}Pr-PNN with $FeCl_2$ or $FeBr_2$ in a 1:1 ratio. The elemental analyses of the red products are in a good agreement with a 1:1 ratio of the ligand and the iron dihalide. Complexes **3** and **4** feature resonances in the paramagnetic region of the ^{1}H NMR spectra. For complex **3**, a solution-state magnetic measurement at ambient temperature is in accordance with an S = 2 spin state with effective magnetic moment of μ_{eff} = 5.3 μ_B. Because of its low solubility, the magnetic susceptibility measurement for **4** was performed in the solid state at 23 °C using a SQUID magnetometer. The measurement, resulting in a magnetic moment of μ_{eff} = 5.20 μ_B, again indicates an S = 2 spin ground state. Characteristic complex ions containing ligand–iron fragments (e.g., [(^{i}Pr-PNN)Fe(X)]$^+$) were detected in the ESI-MS spectra for both complexes.

According to the X-ray diffraction analysis, the *mono*-chelated complex [(^{i}Pr-PNN)Fe(Br)$_2$] **4** is a penta-coordinated iron complex. It is isostructural to complex **2** and features a distorted trigonal bipyramidal iron center (Figure 2, left). The N1–Fe–P angle between the axial atoms is 151.72(6)°. The P-arm of the ligand is not perfectly located in the plane through the bipyridine–iron unit (N1, N2, Fe), and the distances of the benzylic carbon and the phosphorus atom from this plane are 0.5277(26) and 0.2113(6) Å, respectively.

Treatment of either $FeCl_2$ or $FeBr_2$ with a 2-fold excess of ^{i}Pr-PNN in THF initially results in red solutions, and after one or two days of stirring at room temperature the formation of purple precipitates is observed. These solids are insoluble in apolar solvents but are highly soluble in alcohols and acetonitrile. The

dx.doi.org/10.1021/ic401432m | Inorg. Chem. 2013, 52, 9636–9649

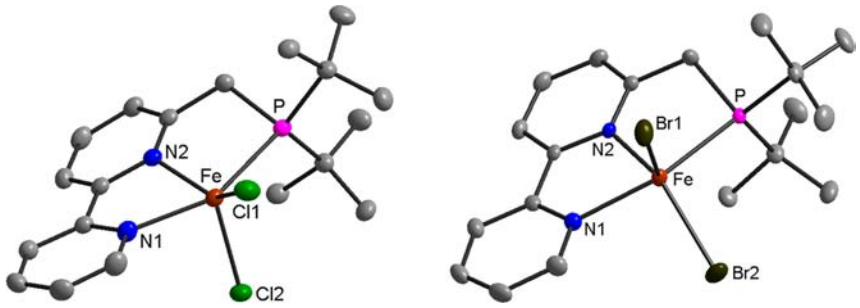

Figure 1. ORTEP diagram of the molecular structure of $[(^{t}\text{Bu-PNN})\text{Fe}(\text{Cl})_2]$ (**1**, left) and $[(^{t}\text{Bu-PNN})\text{Fe}(\text{Br})_2]$ (**2**, right) (ellipsoids set at the 50% probability level). The solvent molecules and hydrogen atoms are omitted for clarity. Bond lengths (Å) and angles (deg): Complex **1**: Fe−N1 2.177(2), Fe−N2 2.2019(19), Fe−P 2.5574(7), Fe−Cl1 2.3082(7), Fe−Cl2 2.3534(6), N1−Fe−N2 73.52(7), N1−Fe−P 151.37(5), N1−Fe−Cl1 95.48(6), N1−Fe−Cl2 89.44(5), N2−Fe−P 78.18(5), N2−Fe−Cl1 142.11(5), N2−Fe−Cl2 108.81(5), P−Fe−Cl1 104.31(2), P−Fe−Cl2 103.87(2), Cl1−Fe−Cl2 107.18(2). Complex **2**: Fe−N1 2.1550(14), Fe−N2 2.2039(13), Fe−P 2.5034(5), Fe−Br1 2.4636(3), Fe−Br2 2.4873(3), N1−Fe−N2 73.97(5), N1−Fe−P 148.57(4), N1−Fe−Br1 96.19(4), N1−Fe−Br2 94.40(4), N2−Fe−P 77.27(4), N2−Fe−Br1 113.17(4), N2−Fe−Br2 139.34(4), P−Fe−Br1 106.669(14), P−Fe−Br2 99.236(13), Br1−Fe−Br2 106.664(11).

Scheme 4. Synthesis of Complexes 3−6 (P = P^{i}Pr$_2$)

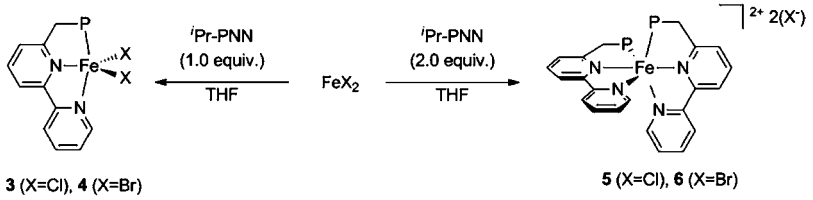

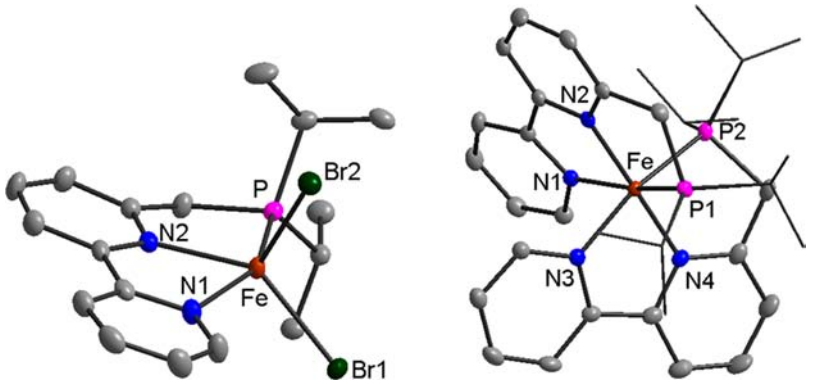

Figure 2. ORTEP diagram of the molecular structure of $[(^{i}\text{Pr-PNN})\text{Fe}(\text{Br})_2]$ (**4**, left) and $[(^{i}\text{Pr-PNN})_2\text{Fe}](\text{Br})_2$ (**6**, right) (ellipsoids set at the 50% probability level). The solvent molecules, hydrogen atoms, and the bromide counterions of **6** are omitted for clarity, while the *iso*-propyl substituents of **6** are shown as thin lines. Bond lengths (Å) and angles (deg): Complex **4**: Fe−N1 2.153(2), Fe−N2 2.2060(19), Fe−P 2.5073(7), Fe−Br1 2.4780(4), Fe−Br2 2.5014(4), N1−Fe−N2 74.14(7), N1−Fe−P 151.72(6), N1−Fe−Br1 96.36(6), N1−Fe−Br2 91.35(5), N2−Fe−P 78.01(5), N2−Fe−Br1 137.88(5), N2−Fe−Br2 113.64(5), P−Fe−Br1 101.021(18), P−Fe−Br2 104.33(2), Br1−Fe−Br2 107.418(15). Complex **6**: Fe−N1 1.995(2), Fe−N2 1.946(2), Fe−N3 1.987(2), Fe−N4 1.940(2), Fe−P1 2.2813(8), Fe−P2 2.2696(8), N1−Fe−N2 80.82(9), N1−Fe−N3 80.63(9), N1−Fe−N4 98.94(9), N1−Fe−P1 163.20(7), N1−Fe−P2 91.45(7), N2−Fe−N3 98.12(9), N2−Fe−N4 179.02(10), N2−Fe−P1 84.24(7), N2−Fe−P2 98.11(7), N3−Fe−N4 80.90(10), N3−Fe−P1 93.98(7), N3−Fe−P2 160.54(7), N4−Fe−P1 95.87(7), N4−Fe−P2 82.84(7), P1−Fe−P2 98.26(3).

^{1}H, ^{13}C{^{1}H}, and ^{31}P{^{1}H} NMR spectra of the resulting diamagnetic complexes $[(^{i}\text{Pr-PNN})_2\text{Fe}](\text{X})_2$ (**5**: X = Cl and **6**: X = Br, Scheme 4) are identical. The ^{31}P{^{1}H} NMR spectra have one resonance at δ = 60.6 ppm. All resonances in the ^{1}H and ^{13}C{^{1}H} NMR spectra were fully assigned by 2D NMR experiments. These spectra show one set of signals for the pincer ligand, containing diastereotopic isopropyl groups. ESI-MS measurements indicate the formation of a *bis*-chelated iron(II) complex, and the results of elemental analyses are in a good agreement with a ligand:iron dihalide ratio of 2:1. In accordance with low-spin ground states (S = 0), no paramagnetic shifts were observed in the magnetic measurements (Evans' method) of both compounds.

X-ray diffraction analysis of **6** shows the formation of the dicationic complex $[(^{i}\text{Pr-PNN})_2\text{Fe}]^{2+}$ with the iron center coordinated to two pincer ligands in a distorted octahedral geometry (Scheme 4 and Figure 2, right). Similar to other examples in the literature,[25] both ^{i}Pr-PNN ligands are coordinated to the Fe^{2+} center in a meridional fashion. The *trans* N−Fe−P angles of the pincer ligands, are 163.20(7) (for N1−Fe−P1) and 160.54(7)° (for N3−Fe−P2), showing significant distortion from the ideal octahedral geometry. The dication $[(^{i}\text{Pr-PNN})_2\text{Fe}]^{2+}$ **6**, featuring an iron(II) center in a low-spin configuration shows, as expected, significantly shorter Fe−N and Fe−P bond distances than found in the iron(II) high-spin complex **4**. The Fe−P distances are 2.51 Å and 2.27−2.28 Å

dx.doi.org/10.1021/ic401432m | Inorg. Chem. 2013, 52, 9636−9649

for the *mono*-chelated and *bis*-chelated complexes **4** and **6**, respectively. The Fe−N distances in *cis*-position to the P atom are 2.21 Å and 1.94−1.95 Å, for **4** and **6**, respectively, and the Fe−N distances in the para-position to the P atom are 2.15 Å and 1.99−2.00 Å

The reactions of the Ph-PNN ligand with $FeCl_2$ and $FeBr_2$ in a 1:1 ratio lead to the formation of intensely orange colored products $[(\text{Ph-PNN})_2\text{Fe}](FeX_4)$ (**7**: X = Cl, and **8**: X = Br, Scheme 5). The resulting complexes are insoluble in THF and CH_2Cl_2, poorly soluble in MeCN, and highly soluble in MeOH. The NMR spectra of **7** and **8** are identical and show resonances in the typical diamagnetic range. The ^1H and $^{13}C\{^1H\}$ NMR spectra exhibit two sets of resonances for the inequivalent phenyl substituents, indicating the absence of a plane of symmetry through the iron pincer moiety. The protons of the methylene group give rise to two distinct resonances with a geminal coupling constant of $^2J_{HH}$ = 17.5 Hz and a coupling constant of $^2J_{PH}$ = 8.1 Hz to the phosphorus atom. The phosphorus resonance appears at δ = 54.4 ppm in the $^{31}P\{^1H\}$ NMR spectrum. Solution-state measurements of the magnetic susceptibility of complexes **7** and **8** at room temperature (Evans' method) resulted in values expected for $S = 2$ complexes. These magnetic moments of μ_{eff} = 5.1 μ_B for complex **7** and **8**, stem from the high-spin FeX_4^{2-} anions.[26] The EI-MS spectra show signals characteristic for iron(II) fragment ions containing one and two pincer ligands (e.g., $[(\text{Ph-PNN})_2\text{Fe}]^{2+}$).

Scheme 5. Synthesis of Complexes 7 and 8 (P = PPh_2)

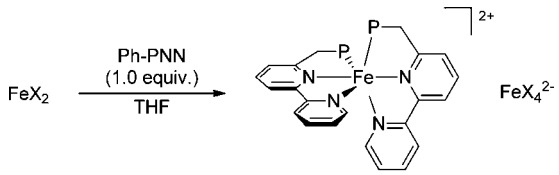

7 (X=Cl), **8** (X=Br)

X-ray diffraction analysis unequivocally confirms the formation $[(\text{Ph-PNN})_2\text{Fe}](FeBr_4)$ (**8**, Figure 3). The dicationic **8** is isostructural to $[(^i\text{Pr-PNN})_2\text{Fe}]^{2+}$ (**6**). The iron atom is coordinated by two pincer ligands in a distorted octahedral geometry. The *trans* N−Fe−P angles of 165.9(3)° (for N1−Fe−P1) and 166.0(3)° (for N3−Fe−P2) are slightly larger than in **6**, while the Fe−N and Fe−P bond distances are almost equal in both dications.

Bipyridine-based ligands (bpy) are known on occasion to be redox noninnocent and can exist in three different oxidation states, namely, as a neutral ligand (bpy^0), as a π-radical monoanion ($bpy^{\bullet-}$), and as a diamagnetic dianion (bpy^{2-}).[27] The one- and two-electron reduction of bipyridine ligands is accompanied by structural changes within the five-membered metallacycle involving a distinct stepwise shortening of the C−C bond connecting the two pyridines. Experimental bond lengths for (bpy^0), ($bpy^{\bullet-}$), and (bpy^{2-}), are approximately 1.49, 1.43, and 1.38 Å, respectively. The interpyridine C−C bond distances of the complexes reported here range from 1.467(4) (for complex **6**) to 1.492(3) Å (for complex **1**) and are indicative of a neutral bipyridine unit in these complexes.

The nature of the substituents of the phosphine moiety determines if *mono*-chelated iron complexes of the type $[(\text{PNN})\text{Fe}(X)_2]$ or *bis*-chelated dications of the type $[(\text{PNN})_2\text{Fe}]^{2+}$ are obtained as products upon reaction of the PNN ligands with FeX_2 (X = Cl, Br) in a 1:1 ratio (Scheme 6).

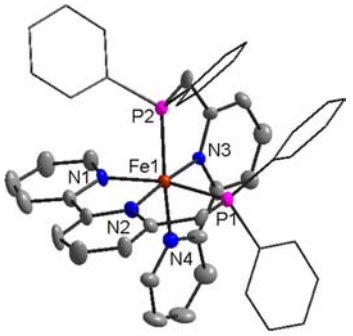

Figure 3. ORTEP diagram of the molecular structure of $[(\text{Ph-PNN})_2\text{Fe}](FeBr_4)$ (**8**) (ellipsoids set at the 50% probability level). The solvent molecules, hydrogen atoms, and the $FeBr_4^{2-}$ counterion are omitted for clarity, while the phenyl substituents are shown as thin lines. Bond lengths (Å) and angles (deg): Fe−N1 1.981(9), Fe−N2 1.936(9), Fe−N3 1.993(10), Fe−N4 1.952(8), Fe−P1 2.249(3), Fe−P2 2.242(3), N1−Fe−N2 82.0(4), N1−Fe−N3 86.2(4), N1−Fe−N4 98.5(4), N1−Fe−P1 165.9(3), N1−Fe−P2 91.4(3), N2−Fe−N3 93.7(4), N2−Fe−N4 175.0(4), N2−Fe−P1 84.7(3), N2−Fe−P2 99.6(3), N3−Fe−N4 81.4(4), N3−Fe−P1 89.8(3), N3−Fe−P2 166.0(3), N4−Fe−P1 94.3(3), N4−Fe−P2 85.4(3), P1−Fe−P2 95.64(12).

While the *tert*-butyl substituted ligand leads exclusively to formation of the paramagnetic complexes **1** and **2** (type **I**, Scheme 6), reactions of the phenyl substituted ligand lead exclusively to complexes **7** and **8**, which contain the diamagnetic dication $[(\text{Ph-PNN})_2\text{Fe}]^{2+}$ (type **II**, Scheme 6) with FeX_4^{2-} counteranions. With the *iso*-propyl substituted ligand, both types of complexes are obtained depending on the initial reaction conditions.

Scheme 6. *Mono*-Chelated Iron Dihalide Complexes (I) and *bis*-Chelated Dications (II)[a]

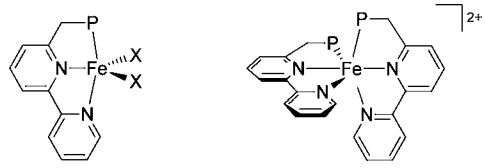

I II

[a] X = Cl or Br, and P = PR_2.

To gain additional insight, we performed DFT calculations to compare the relative energies of the reactions leading to the complexes type **I** and **II** (Scheme 6). Geometries were optimized at the DF-PBE/SVP level of theory, and energies were calculated, using a double hybrid functional employing a solvation model (MeOH) at 298 K (see Computational Details section for full details). For the iron complexes, all possible spin states were considered. In accordance with the magnetic measurements, the *mono*-chelated complexes of the type **I** and the FeX_4^{2-} anions were found to have quintet ground states (S = 2), while the dicationic 18-electron complexes of the type **II** have singlet ground states (S = 0).

For the ^{t}Bu-PNN ligand, only type **I** complexes (i.e., complexes **1** and **2**) were observed experimentally. This can be explained by the steric bulk of the P^tBu_2 moiety, the pincer ligand being too large to allow for two ligands to bind to the iron center. When trying to build the geometry of isomer **II** for the ^{t}Bu-PNN ligand, it became readily apparent that it is not possible for two

dx.doi.org/10.1021/ic401432m | Inorg. Chem. 2013, 52, 9636−9649

ligands to be bound to the iron center without the methyl groups of the two ^{t}Bu substituents overlapping.

The reactions of the *mono*-chelated ^{i}Pr-PNN complexes **3** and **4** with an additional ligand ^{i}Pr-PNN (leading to the formation of the *bis*-chelated complexes **5** and **6**) are calculated to be slightly endergonic, by 6.4 and 10.7 kcal/mol, respectively (Scheme 7). This is in agreement with the clean formation of [(^{i}Pr-PNN)Fe(X)$_2$] from 1:1 mixtures of FeX_2 and ^{i}Pr-PNN. However, the salts **5** and **6**, formed in reactions with an excess of ^{i}Pr-PNN, are insoluble in THF, and the lattice energy, which is not considered in the calculations, helps to drive the reactions toward the products. In the case of the Ph-PNN ligand, the experiments show that formation of the salts [(Ph-PNN)$_2$Fe]-(FeX_4) (**7** and **8**) is favored over formation of the *mono*-chelated complexes [(Ph-PNN)Fe(X)$_2$]. The difference in ΔG_{298} was calculated to be 3.3 kcal/mol for the chloride complex **7** and 0.0 kcal/mol for the bromide complex **8** in favor of the salts (Scheme 7), not considering the additional stabilization provided by the lattice energy of the precipitated salts.

Scheme 7. Calculated Gibbs Energies [kcal/mol] of the Reactions Leading to the Formation of 5−8[a]

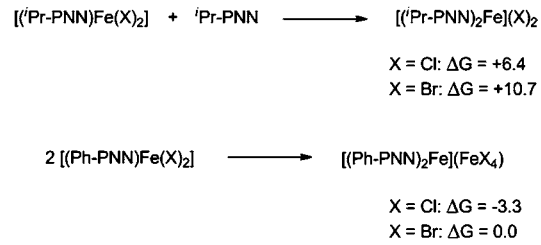

[a] $\Delta G_{298,MeOH}$ given at the SMD(MeOH)-DSD-PBEP86/TZVP//DF-PBE/SVP/SVPfit level of theory.

The *bis*-chelated dicationic complexes of the type $[(PNN)_2Fe]^{2+}$ readily undergo deprotonation of the benzylic arms upon reaction with different bases, such as MeLi, KO^{t}Bu, or LiHMDS. The doubly dearomatized complexes [(^{i}Pr-PNN*)$_2$Fe] (**9**) and [(Ph-PNN*)$_2$Fe] (**10**) were synthesized with concomitant formation of KBr and HO^{t}Bu (and $FeBr_2$ or $K_2[FeBr_4]$ for **10**) by treatment of the complexes **6** and **8** with 2 equiv of KO^{t}Bu in dry THF for 8 h (Scheme 8). These complexes are diamagnetic and, in contrast to the starting materials, are soluble in THF, toluene, and benzene.

Complexes **9** and **10** were characterized by multinuclear NMR spectroscopy; all resonances in the ^{1}H and ^{13}C{^{1}H} NMR spectra were fully assigned by 2D-NMR measurements. Both complexes have two sets of inequivalent substituents on the phosphorus atoms in the ^{1}H and ^{13}C{^{1}H} NMR spectra. The benzylic protons integrate to 1 H per pincer ligand and are

Scheme 8. Deprotonation Reactions Resulting in the Dearomatized Complexes 9 and 10

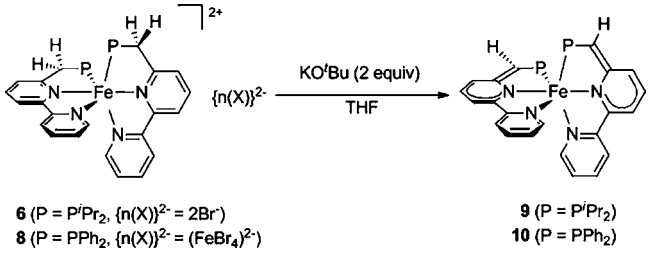

observed as broad resonances at δ = 4.03 (for complex **9**) and 4.43 ppm (for complex **10**) in the ^{1}H and ^{1}H{^{31}P} NMR spectra. The resonances of the benzylic carbon atoms were observed as multiplets centered at δ = 67.2 and 60.7 ppm in the ^{13}C{^{1}H} NMR spectra of **9** and **10** respectively. The ^{31}P{^{1}H} NMR spectra contain singlets at δ = 51.8 and 50.6 ppm for complex **9** and **10**, respectively.

^{1}H-^{15}N-HMQC NMR measurements were performed for complexes **6**, **8**, **9**, and **10** to compare the chemical shifts of the bipyridine nitrogen atoms of these complexes (see Table 1 and Supporting Information). The deprotonation reactions lead to distinct shifts of the ^{15}N resonances of the central pyridine rings (N2) to significantly higher fields and slightly less pronounced shifts of the nitrogen signals of the terminal pyridines (N1) to lower fields.

Table 1. ^{15}N Chemical Shifts [ppm] of Complexes 6, 8, 9, and 10 Obtained by ^{1}H-^{15}N-HMQC NMR Measurements (41 MHz, 23 °C)

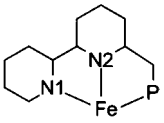

	complex **6**[a]	complex **8**[a]	complex **9**[b]	complex **10**[c]
N1	254.7	256.8	273.2	269.5
N2	260.7	254.9	199.7	204.7

[a] Spectrum measured in CD_3OD. [b] Spectrum measured in C_6D_6. [c] Spectrum measured in toluene-d_8.

The structure of complex **10** was unequivocally confirmed by X-ray diffraction analysis (Figure 4), which shows a neutral complex with the iron center coordinated by two deprotonated pincer ligands in a distorted octahedral fashion. A comparison of this structure with the structure of the dication **8** reveals distinct changes in the bond distances resulting from the deprotonation of the benzylic arms of the ligands. While deprotonation does not significantly affect the coordination sphere around the iron center, differences in the bond distances are observed within the pincer ligands. Table 2 summarizes the bond distances in the pincer ligands of **8** and **10**. The bond distances of the benzylic carbon atom (C11) to the pyridine *ipso* carbon atom (C10) and to the phosphorus atom decrease by 0.114 and 0.087 Å, respectively. The average of the benzylic C−C_{ipso} bond distances is 1.504 Å (for **8**) and 1.390 Å (for **10**) and the average C−P bond distance decreases from 1.839 Å (for **8**) to 1.752 Å (for **10**). The shortening of these bonds is accompanied by an elongation of the bonds to the *ipso* carbon atom (C10) within the pyridine ring. The averaged C9−C10 bond distance changes from 1.386 Å (for **8**) to 1.433 Å (for **10**) and the C10−N2 bond from 1.358 Å (for **8**) to 1.390 Å (for **10**). This suggests a strong double bond character between C10 and C11. These values are in the range reported for dearomatized pyridine-based metal complexes.[28] It is noteworthy that this is, to our knowledge, the first example of a structurally characterized metal complex featuring a deprotonated bipyridine-based pincer ligand and, furthermore, the first example of a dearomatized iron pincer complex.

Metal−ligand cooperation by ligand aromatization-dearomatization of transition metal complexes featuring pyridine-based pincer ligands is of importance in bond activation reactions and catalytic processes.[29] It has been shown that dearomatized complexes are capable of activating of H−H, C−H (sp^2 and sp^3),

dx.doi.org/10.1021/ic401432m | Inorg. Chem. 2013, 52, 9636−9649

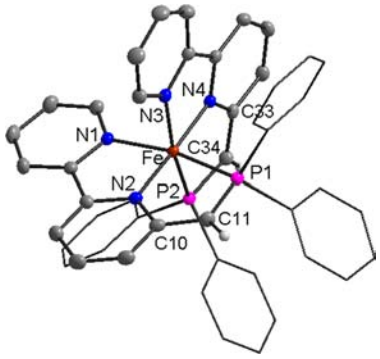

Figure 4. ORTEP diagram of the molecular structure of [(Ph-PNN*)$_2$Fe] (**10**) (ellipsoids set at the 50% probability level). The solvent molecules and all hydrogen atoms, other than those on the PNN ligand arms, are omitted for clarity, while the phenyl substituents are shown as thin lines. Bond lengths (Å) and angles (deg): Fe–N1 1.9690(13), Fe–N2 1.9383(12), Fe–N3 1.9820(13), Fe–N4 1.9410(12), Fe–P1 2.2380(4), Fe–P2 2.2231(4), C10–C11 1.387(2), C33–C34 1.393(2), N1–Fe–N2 80.65(5), N1–Fe–N3 90.43(5), N1–Fe–N4 99.40(5), N1–Fe–P1 165.21(4), N1–Fe–P2 88.64(4), N2–Fe–N3 95.01(5), N2–Fe–N4 175.58(5), N2–Fe–P1 84.60(4), N2–Fe–P2 99.85(4), N3–Fe–N4 80.57(5), N3–Fe–P1 89.80(4), N3–Fe–P2 164.75(4), N4–Fe–P1 95.22(4), N4–Fe–P2 84.57(4), P1–Fe–P2 94.959(16).

Table 2. Comparison of Bond Lengths [Å] between the Aromatized Dication of 8 and the Doubly Dearomatized Complex 10[a]

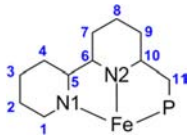

	[(Ph-PNN)$_2$Fe]$^{2+}$ (**8**)		[(Ph-PNN*)$_2$Fe] (**10**)	
bond	ligand 1	ligand 2	ligand 1	ligand 2
Fe–P	2.249(3)	2.242(3)	2.2380(4)	2.2231(4)
Fe–N1	1.981(9)	1.993(10)	1.9690(13)	1.9820(13)
Fe–N2	1.936(9)	1.952(8)	1.9383(12)	1.9410(12)
C1–C2	1.409(18)	1.398(18)	1.377(2)	1.384(2)
C2–C3	1.358(19)	1.35(2)	1.391(2)	1.386(2)
C3–C4	1.394(19)	1.41(2)	1.382(2)	1.382(2)
C4–C5	1.397(16)	1.393(18)	1.391(2)	1.392(2)
C5–C6	1.484(15)	1.478(16)	1.469(2)	1.467(2)
C6–C7	1.377(16)	1.399(15)	1.383(2)	1.383(2)
C7–C8	1.407(18)	1.392(18)	1.405(2)	1.398(2)
C8–C9	1.380(18)	1.390(17)	1.366(2)	1.372(2)
C9–C10	1.377(15)	1.395(15)	1.433(2)	1.433(2)
C10–C11	1.516(15)	1.492(15)	1.387(2)	1.393(2)
N1–C1	1.339(15)	1.331(15)	1.350(2)	1.3451(19)
N1–C5	1.351(14)	1.374(15)	1.3616(19)	1.3609(19)
N2–C6	1.355(14)	1.348(14)	1.357(2)	1.3580(19)
N2–C10	1.357(14)	1.359(13)	1.3895(19)	1.3880(19)
P–C11	1.842(11)	1.835(11)	1.7508(16)	1.7525(15)

[a]Ligands 1 and 2 refer to the crystallographically inequivalent pincer ligands of the *bis*-chelated complexes.

O–H, and N–H bonds without changing the formal oxidation state of the metal. Dearomatized complexes can activate these E-H bonds by cooperation between the metal and the ligand, thereby regaining aromatization of the ligand by protonation of the benzylic carbon atom. These reactions are usually accompanied by the coordination of E^- to the metal center. This coordination might be, in many cases, an additional driving force for these activation reactions. It, however, cannot take place on coordinatively saturated complexes, unless one ligand dissociates.

Thus, it is not surprising that the dearomatized complexes **9** and **10** do not react with H_2 (under 2 atm. pressure) or with an excess of hexylamine (~400 equiv). However, the complexes are readily protonated by an excess of methanol or water (Scheme 9). A comparison of both complexes in these experiments suggests that the *iso*-propyl-substituted complex **9** is more basic than the phenyl-substituted complex **10**.

Scheme 9. Protonation Reactions of 9 and 10

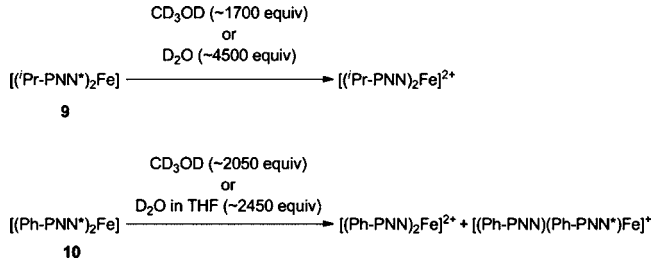

Dissolving **9** in CD_3OD (~1700 equiv) or D_2O (~4500 equiv) leads to formation of intensely red solutions and full conversions to [(^{i}Pr-PNN)$_2$Fe]$^{2+}$ as observed by NMR spectroscopy. However, dissolving **10** in CD_3OD (~2050 equiv) results in the formation of a roughly 1:1 mixture of the doubly protonated dicationic complex [(Ph-PNN)$_2$Fe]$^{2+}$ and the singly protonated complex [(Ph-PNN)(Ph-PNN*)Fe]$^+$. The mono-cationic complex [(Ph-PNN)(Ph-PNN*)Fe](PF_6) (**12**) was alternatively synthesized by reaction of the doubly deprotonated complex [(Ph-PNN*)$_2$Fe] (**10**) with 1 equiv of the doubly protonated complex [(Ph-PNN)$_2$Fe](PF_6)$_2$ (**11**) in THF (Scheme 10). Complex **12** can also be obtained by deprotonation of **11** with 1 equiv KO^{t}Bu in MeCN. The mono-dearomatized complex **12** exhibits a characteristic AB system in the $^{31}P\{^1H\}$ NMR spectrum with two doublets located at δ = 61.5 and 43.9 ppm featuring a coupling constant of $^2J_{PP}$ = 47.6 Hz. The dearomatized pincer ligand features a broad singlet at δ = 4.03 for the benzylic hydrogen atom in the ^1H NMR spectrum, and the aromatized ligand shows two resonances at δ = 3.74 and 4.54 ppm for the diastereotopic benzyl hydrogen atoms with a geminal coupling of $^2J_{HH}$ = 18.0 Hz.

The addition of D_2O (~4650 equiv) to complex **10** results in the formation of a suspension that consists of an orange colored solution and a dark precipitate. Increasing the amount of D_2O to approximately 12500 equiv does not completely dissolve the

Scheme 10. Synthesis of Complexes 11 and 12 (P = PPh_2)

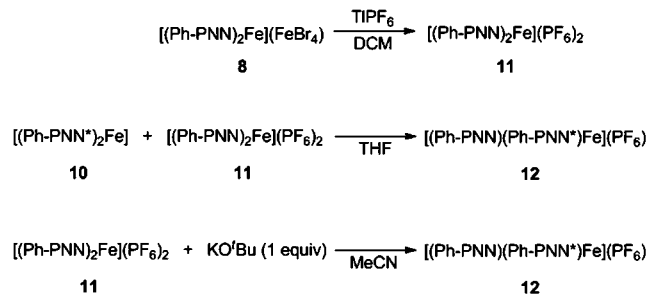

dx.doi.org/10.1021/ic401432m | Inorg. Chem. 2013, 52, 9636–9649

precipitate. In solution, only the dication $[(\text{Ph-PNN})_2\text{Fe}]^{2+}$ was observed by NMR spectroscopy. However, carrying out the reaction of **10** with an excess of D_2O (~2450 equiv) in THF results in the formation of an intensely greenish-brown solution. ^1H and $^{31}P\{^1H\}$ NMR measurements show the formation of $[(\text{Ph-PNN})_2\text{Fe}]^{2+}$ and $[(\text{Ph-PNN})(\text{Ph-PNN*})\text{Fe}]^{+}$ in a mixture of roughly 1:6.

The protonation reaction of complex **10** with CD_3OD is fully reversible. Evaporation of the solvent from the reaction of **10** with CD_3OD and exposure of the residue to high vacuum leads to full conversion to the doubly dearomatized complex **10**. This reaction is accompanied by a change in color from redish-brown to brown. Partial deuterium incorporation into the benzylic positions was observed by ^2D NMR, and the integration of the residual resonance of benzylic proton in the ^1H NMR spectrum gives about 0.7 H per pincer ligand. The $^{31}P\{^1H\}$ NMR spectrum of the resulting mixture of differently deuterated complexes shows a multiplet (see Supporting Information). The multiplet consists of the two superimposed resonances of the non-deuterated complex $\mathbf{10}^{\mathbf{HH}}$, which exhibits a singlet at δ = 50.5 ppm, and the *mono*-deuterated complex $\mathbf{10}^{\mathbf{HD}}$, which shows a symmetrical multiplet centered at δ = 50.4 ppm resulting from second order spin coupling of the AA′X system.

To obtain a higher percentage of deuteration, CD_3OD (~1900 equiv) was added to **10** and evaporated. Repeating this procedure five times resulted in 85% deuteration of the complex in the benzylic position. The $^{31}P\{^1H\}$ NMR spectrum (see Supporting Information) of the complex mixture shows a second order spin system of a *mono*-deuterated complex $\mathbf{10}^{\mathbf{HD}}$ that is superimposed with a broad singlet at δ = 50.4 ppm of the doubly deuterated complex $\mathbf{10}^{\mathbf{DD}}$.

As with **10**, evaporation of all volatiles from the reaction of **9** with CD_3OD results in a change of color from red to brown. Extraction of the resulting brown solid with toluene-d_8 gives a brown solution and an insoluble, unidentified, green residue. The ^1H and $^{31}P\{^1H\}$ NMR spectra of the solution show formation of minor amounts **9** along with major amounts of the *mono*-deuterated free ligand. The $^{31}P\{^1H\}$ NMR spectrum exhibits a multiplet for **9**, similar to **10**. The integration of this multiplet with respect to the pseudo triplet resonance of the *mono*-deuterated ligand (δ = 11.2 ppm; $^2J_{PD}$ = 42.2 Hz) in the $^{31}P\{^1H\}$ NMR spectrum gave a ratio **9** to the free ligand of approximately 1:7.

CONCLUSIONS

In summary, bipyridine-based PNN-type iron pincer complexes were readily prepared from reactions of bipyridine-based PNN ligands with FeX_2 (X = Cl and Br). Three different ligands, the known ^{t}Bu-PNN ligand and the new ^{i}Pr-PNN and Ph-PNN, were studied in this work. Depending on the ratios between the ligand and metal salt, and on the PR_2 substituents, three different types of complexes were obtained. Reactions of the most bulky ligand ^{t}Bu-PNN with FeX_2 give the *mono*-chelated, paramagnetic, high-spin complexes $[(^t\text{Bu-PNN})\text{Fe}(X)_2]$ **1** and **2**, exclusively. The analogous complexes $[(^i\text{Pr-PNN})\text{Fe}(X)_2]$ **3** and **4** are obtained in reactions with ^{i}Pr-PNN when the ligand and FeX_2 are reacted in a 1:1 ratio. Increasing this ratio to 2:1, or reacting $[(^i\text{Pr-PNN})\text{Fe}(X)_2]$ with an additional equivalent of the ligand, leads to formation of the dicationic, *bis*-chelated, diamagnetic, low-spin complexes $[(^i\text{Pr-PNN})_2\text{Fe}](X)_2$ (**5** and **6**). DFT calculations show that the second ligation step is slightly endergonic, but the reactions are driven by the formation of the insoluble salts. Reactions of FeX_2 with Ph-PNN in a 1:1 ratio yield the *bis*-chelated salts $[(\text{Ph-PNN})_2\text{Fe}](FeX_4)$ (**7** and **8**). The formation of **7** and **8** is thermodynamically favored over the formation of the *mono*-chelated complexes $[(\text{Ph-PNN})\text{Fe}(X)_2]$. The *bis*-chelated dication $[(\text{Ph-PNN})_2\text{Fe}]^{2+}$ in these salts is isostructural with the ^{i}Pr substituted dication. The *bis*-chelated dicationic complexes $[(^i\text{Pr-PNN})_2\text{Fe}]^{2+}$ and $[(\text{Ph-PNN})_2\text{Fe}]^{2+}$ undergo deprotonation of the benzylic carbon atoms in the presence of suitable bases. The doubly deprotonated complexes $[(^i\text{Pr-PNN*})_2\text{Fe}]$ (**9**) and $[(\text{Ph-PNN*})_2\text{Fe}]$ (**10**) were synthesized by reactions of **6** and **8** with KO^{t}Bu. The structural analysis of **10** unequivocally confirms the resulting dearomatization of the pincer ligands. These complexes are reversibly protonated in the presence of an excess of water or methanol, and the reactions performed suggest that complex **9** is more basic than complex **10**.

A very recent report by Huang et al. on the application of complex **1** as precatalyst for hydroboration reactions[22] indicates the high catalytic potential of these compounds. Studies of the scope of complexes **1**−**4** in different catalytic reactions are currently underway in our laboratories.

EXPERIMENTAL SECTION

General Considerations. All reactions were performed under a nitrogen atmosphere in a glovebox or using standard Schlenk techniques. All solvents were reagent grade or better. Tetrahydrofuran, benzene, toluene, diethylether, and pentane were refluxed over sodium and distilled under an argon atmosphere. Methylene chloride, methanol, and acetonitrile were degassed by freeze-pump thaw cycles and stored in the glovebox over the appropriate molecular sieves. Deuterated solvents were sparged with argon and stored in the glovebox over the appropriate molecular sieves. Other commercially available reagents were used as received.

NMR spectra were recorded using Bruker AMX-300, AMX-400, and AMX-500 NMR spectrometers. ^1H and $^{13}C\{^1H\}$ NMR chemical shifts are reported in ppm downfield from tetramethylsilane. $^{31}P\{^1H\}$ NMR chemical shifts are reported in ppm downfield from H_3PO_4 (0.0 ppm) and are referenced to an external 85% solution of phosphoric acid in D_2O. NMR assignments (Scheme 11) of the diamagnetic compounds were assisted by ^1H-^1H-COSY, ^1H-^{31}P-HMQC, ^1H-^{13}C-HSQC, ^1H-^{13}C-HMBC, and ^{13}C-DEPTQ NMR spectroscopy, as required. ^{15}N chemical shifts were identified by ^1H-^{15}N-HMQC NMR measurements and are reported downfield from liquid ammonia (0.0 ppm). ^1H NMR spectra of the paramagnetic compounds were recorded with a d_1 time of 50 ms, from samples of approximately 2 mg substance in 0.6 mL of solvent. The effective magnetic moments in solution were measured by the Evans' method[23] at ambient temperature. The measurement of the magnetic susceptibility of a sample of complex **4** (20.7 mg powder) was performed on a Quantum design MPMS XL SQUID magnetometer, employing a field of 3000 Oe. IR spectra were recorded on a Nicolet FT-IR spectrophotometer. Elemental analyses and ESI-MS spectroscopy were performed by the Department of Chemical Research Support, Weizmann Institute of Science.

Synthesis of PNN Ligands. 6-Chloromethyl-2,2′-bipyridine was prepared according to the literature.[30]

Scheme 11. Assignment of the Carbon and Hydrogen Atoms of the PNN Ligands

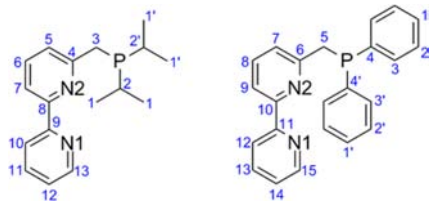

dx.doi.org/10.1021/ic401432m | Inorg. Chem. 2013, 52, 9636−9649

^{t}Bu-PNN (6-Di-tert-butylphosphinomethyl-2,2′-bipyridine). This was prepared as reported previously.[13]

^{i}Pr-PNN (6-Di-iso-propylphosphinomethyl-2,2′-bipyridine). A pressure vessel was charged with a mixture of 6-chloromethyl-2,2′-bipyridine (1.03 g, 5.00 mmol), di-*iso*-propyl phosphine (710 mg, 6.00 mmol), and MeOH (15 mL). The reaction mixture was heated to 50 °C for 48 h with stirring. The reaction mixture was allowed to reach room temperature, and triethylamine (910 mg, 9.00 mmol) was added. After stirring the reaction mixture at room temperature for 1 h, all volatiles were removed in vacuo. The crude product was extracted from the colorless residue with ether (2 × 10 mL). Upon evaporation of the ether in vacuo a pale yellow liquid was obtained. The product was purified by column chromatography over basic alumina using hexane as eluent to yield 874 mg (61%) of a pale yellow liquid. **Anal. Calcd. (found)** for $C_{17}H_{23}N_2P$ [286.16 g·mol^{-1}]: C 71.30 (71.52), H 8.10 (8.34). **ESI-MS**: 309.16 (M + Na$^+$, $C_{17}H_{23}N_2PNa^+$), 287.16 (M + H$^+$, $C_{17}H_{24}N_2P^+$). **^{1}H NMR** (400 MHz, CD_2Cl_2, 23 °C): δ = 1.11 (dd, 6 H, $^3J_{PH}$ = 13.8 Hz, $^3J_{HH}$ = 7.2 Hz, ^{i}Pr−CH_3^A), 1.17 (dd, 6 H, $^3J_{PH}$ = 14.4 Hz, $^3J_{HH}$ = 7.2 Hz, ^{i}Pr−CH_3^B), 1.89 (m, 2 H, ^{i}Pr−C*H*), 3.30 (d, 2H, $^2J_{PH}$ = 1.8 Hz, PCH_2), 7.73 (vt, 1 H, $^3J_{HH}$ = 7.8 Hz *H*6), 7.82 (dvt, 1 H, $^3J_{HH}$ = 7.8 Hz, $^4J_{HH}$ = 1.8 Hz, *H*11), 8.21 (d, 1H, $^3J_{HH}$ = 7.8 Hz, *H*7), 8.46 (d, br, 1H, $^3J_{HH}$ = 8.1 Hz, *H*10), 8.68 (m, 1H, *H*13) ppm. **^{13}C{^{1}H} NMR** (100 MHz, CD_2Cl_2, 23 °C): δ = 18.9 (d, $^2J_{PC}$ = 10.5 Hz, ^{i}Pr-CH_3^A), 19.6 (d, $^2J_{PC}$ = 15.0 Hz, ^{i}Pr-CH_3^B), 23.6 (d, $^1J_{PC}$ = 15.0 Hz, PCH_2), 32.5 (d, br, $^1J_{PH}$ = 22.5 Hz, ^{i}Pr-CH), 117.6 (s, *C*7), 120.8 (s, *C*10), 123.5 (s, *C*12), 123.6 (s, *C*5), 136.7 (s, *C*11), 136.9 (s, *C*6), 149.1 (s, *C*13), 155.2 (s, *C*8), 156.4 (s, *C*9), 161.39 (d, $^2J_{PC}$ = 9.0 Hz, *C*4) ppm. **^{31}P{^{1}H} NMR** (162 MHz, CD_2Cl_2, 23 °C): δ = 15.8 (s) ppm.

Ph-PNN (6-Diphenylphosphinomethyl-2,2′-bipyridine). A Schlenk flask equipped with a reflux condenser and a dropping funnel was charged with a solution of diphenylphosphine in ether (30 mL). The solution was cooled to 0 °C, and a solution of potassium *tert*-butoxide (74 mg, 6.6 mmol) in THF (5 mL) was added dropwise during a period of 10 min. The resulting brown colored mixture was stirred for 1 h at 0 °C, and a solution of 6-chloromethyl-2,2′-bipyridine (1.02 g, 5 mmol) in ether (20 mL) was added dropwise during a period of 10 min. Upon complete addition the reaction mixture was stirred at 0 °C for 1 h and was allowed to reach room temperature overnight. Degassed water (20 mL) was added, and the organic phase was separated under nitrogen. The water phase was extracted with ether (2 × 20 mL), the organic fractions were combined, dried over Na_2SO_4, and filtered. The solvent was removed in vacuo to yield a brownish solid. The crude product was purified by column chromatography over basic alumina using a hexane/ether mixture (10:1) as eluent to yield 1.08 g (61%) of colorless crystals. **Anal. Calcd. (found)** for $C_{17}H_{23}N_2P$ [354.13 g·mol^{-1}]: C 78.13 (77.95), H 5.61 (5.40). **ESI-MS**: 377.08 (M + Na$^+$, $C_{23}H_{19}N_2PNa^+$), 355.20 (M + H$^+$, $C_{23}H_{20}N_2P^+$). **^{1}H NMR** (300 MHz, CD_2Cl_2, 23 °C): δ = 3.81 (s, 2H, P−CH_2), 7.13 (d, $^3J_{HH}$ = 7.5 Hz, 1H, *H*7), 7.32 (m, 1H, *H*14), 7.43 (m, 6H, Ph-*H*), 7.60 (m, 4H, Ph-*H*), 7.69 (vt, 1H, $^3J_{HH}$ = 7.8 Hz, 1H, *H*8), 7.80 (dvt, 1H, $^3J_{HH}$ = 7.8 Hz, $^4J_{HH}$ = 2.1 Hz, *H*-13′), 8.28 (d, br, 2H, J_{HH} = 8,0 Hz, *H*9 + 12), 8.69 (m, 1H, *H*15) ppm. **^{13}C{^{1}H} NMR** (100 MHz, CD_2Cl_2, 23 °C): δ = 38.4 (d, $^1J_{PC}$ = 16.3 Hz, PCH_2), 118.1 (s, *C*9), 121.0 (s, *C*12), 123.5 (s, *C*14), 123.6 (d, J_{PC} = 8.4 Hz, *C*7), 128.3 (s, Ph-*C*), 128.4 (s, Ph-*C*), 128.7 (s, Ph-*C*), 132.9 (s, Ph-*C*), 133.1 (s, Ph-*C*), 136.6 (s, *C*13), 137.0 (s, *C*8), 138.7 (d, J_{PC} = 15.0 Hz, Ph-C_{ipso}), 149.0 (s, *C*13), 155.5 (s, *C*10), 156.2 (s, *C*11), 157.6 (d, J_{PC} = 7.5 Hz, *C*6) ppm. **^{31}P{^{1}H} NMR** (162 MHz, CD_2Cl_2, 23 °C): δ = −8.3 (s) ppm.

Synthesis of Complexes 1−12. *[(^{t}Bu-PNN)Fe(Cl)$_2$] (1).* A solution of ^{t}Bu-PNN (160 mg, 0.51 mmol) in 3 mL of THF was added to a suspension of $FeCl_2$ (63.4 mg, 0.50 mmol) in 12 mL of THF. Upon addition the reaction mixture turned red. After heating the suspension for 5 h to 65 °C, 80 mL of hexane were added. The resulting suspension was filtered, and the residue was dried in vacuo to yield 190 mg (86%) of a red powder. Single crystals of **1** were obtained by slow diffusion of pentane into a saturated solution in methylene chloride. **Anal. Calcd. (found)** for $C_{19}H_{27}Cl_2FeN_2P$ [440.06 g·mol^{-1}]: C 51.73 (51.80), H 6.17 (6.23), N 6.35 (6.29). **ESI-MS**: (*m*/*z*, pos.): 405.10 ([(^{t}Bu-PNN)FeCl]$^+$ = M-Cl$^-$ = $C_{19}H_{27}ClFeN_2P^+$). **^{1}H NMR** (300 MHz, CD_3CN, 23 °C) δ = −15.76, 8.75, 14.38, 23.8, 53.56, 54.14, 76.79, 80.58, 128.43 ppm. No resonance was detected in the ^{31}P{^{1}H} NMR spectrum in a range from −4000 to 4000 ppm. **Magnetic susceptibility** (Evans): μ_{eff} = 5.0 μ_B (1,4-dioxane in $CDCl_3$, 23 °C).

[(^{t}Bu-PNN)Fe(Br)$_2$] (2). A solution of ^{t}Bu-PNN (228 mg, 0.726 mmol) in 3 mL of THF was added to a solution of $FeBr_2$ (153 mg, 0.716 mmol) in 20 mL of THF. Immediately after addition the reaction mixture turned black. After 16 h of stirring at room temperature, the resulting black suspension was layered with pentane (60 mL). The suspension was filtered, the residue was washed with pentane (10 mL), and dried in vacuo to yield 360 mg (95%) of a black powder. Single crystals of **2** were obtained by cooling a saturated solution in acetonitrile to −20 °C. **Anal. Calcd. (found)** for $C_{19}H_{27}Br_2FeN_2P$ [530.06 g·mol^{-1}]: C 43.05 (43.25), H 5.13 (5.25), N 5.28 (5.27). **ESI-MS**: (*m*/*z*, pos.): 449.04 ([(^{t}Bu-PNN)FeBr]$^+$ = M-Br$^-$ = $C_{19}H_{27}BrFeN_2P^+$); (*m*/*z*, neg.): 80.90 (Br$^-$). **^{1}H NMR** (300 MHz, CD_3CN, 23 °C) δ = −13.02, 7.56, 10.17, 15.75, 53.91, 55.99, 77.82, 87.44, 116.50 ppm. No resonance was detected in the ^{31}P{^{1}H} NMR spectrum in a range from −4000 to 4000 ppm. **Magnetic susceptibility** (Evans): μ_{eff} = 5.3 μ_B (1,4-dioxane in $CDCl_3$, 23 °C).

[(^{i}Pr-PNN)Fe(Cl)$_2$] (3). A solution of ^{i}Pr-PNN (57.3 mg, 0.20 mmol) in 3 mL of THF was added to a suspension of $FeCl_2$ (25.2 mg, 0.20 mmol) in 7 mL of THF. Upon addition the reaction mixture turned red. After 16 h of stirring at room temperature, the resulting red suspension was layered with pentane (10 mL). The suspension was filtered, the residue was washed with pentane (20 mL), and dried in vacuo to yield 73.8 mg (89%) of a red powder. **Anal. Calcd. (found)** for $C_{17}H_{23}Br_2FeN_2P$ [413.10 g·mol^{-1}]: C 49.43 (49.72), H 5.62 (5.65), N 6.78 (6.62). **ESI-MS:** (*m*/*z*, pos.): 377.08 ([(^{i}Pr-PNN)Fe(Cl)]$^+$ = $C_{17}H_{23}ClFeN_2P^+$), 170.97 ([(^{i}Pr-PNN)Fe]$^{2+}$ = $C_{17}H_{23}FeN_2P^{2+}$). The compound is paramagnetic and shows 12 resonances in the ^{1}H NMR: **^{1}H NMR** (300 MHz, CD_3CN, 23 °C) δ = −17.99, 0.74, 7.56, 8.65, 8.81, 9.01, 29.96, 51.09, 54.37, 79.88, 80.17, 117.03, 134.25 ppm. No resonance was detected in the ^{31}P{^{1}H} NMR spectrum in a range from −4000 to 4000 ppm. **Magnetic susceptibility** (Evans): μ_{eff} = 5.3 μ_B (1,4-dioxane in $CDCl_3$, 23 °C).

[(^{i}Pr-PNN)Fe(Br)$_2$] (4). A solution of ^{i}Pr-PNN (57.3 mg, 0.20 mmol) in 3 mL of THF was added to a solution of $FeBr_2$ (43.0 mg, 0.20 mmol) in 7 mL of THF. Upon addition a black suspension was formed. After 16 h of stirring at room temperature, the resulting red suspension was layered with pentane (10 mL). The suspension was filtered, the residue was washed with pentane (20 mL), and dried in vacuo to yield 98.7 mg (99%) of a red powder. Single crystals of **4** were obtained by slow evaporation of the solvent from a saturated solution in methylene chloride. **Anal. Calcd. (found)** for $C_{17}H_{23}Br_2FeN_2P$ [502.00 g·mol^{-1}]: C 40.67 (40.69), H 4.62 (4.49), N 5.58 (5.44). **ESI-MS:** (*m*/*z*, pos.): 421.02 ([(^{i}Pr-PNN)Fe(Br)]$^+$ = $C_{17}H_{23}BrFeN_2P^+$), 314.11 ([(^{i}Pr-PNN)$_2$Fe]$^{2+}$ = $C_{34}H_{46}FeN_4P_2^{2+}$), 170.97 ([(^{i}Pr-PNN)Fe]$^{2+}$ = $C_{17}H_{23}FeN_2P^{2+}$); (*m*/*z*, neg.): 78.94 (Br$^-$). NMR spectroscopy of the red powder shows a paramagnetic compound (with 12 resonances in the ^{1}H NMR). **^{1}H NMR** (400 MHz, CD_2Cl_2, 23 °C) δ = −17.16, 1.27, 10.32, 10.55, 10.92, 18.67, 51.71, 57.49, 81.56, 87.42, 120.57, 131.01 ppm. **Magnetic susceptibility** (SQUID): μ_{eff} = 5.20 μ_B (23 °C).

[(^{i}Pr-PNN)$_2$Fe](Cl)$_2$ (5). A solution of ^{i}Pr-PNN (21.0 mg, 73.3 mmol) in 1 mL of THF was added to a solution of $FeBr_2$ (5.0 mg, 23.4 mmol) in 4 mL of THF. Upon addition a black suspension was formed. Pentane (15 mL) was added to the purple suspension after 72 h of stirring at room temperature. The suspension was filtered, the residue was washed with pentane (20 mL) and dried in vacuo to yield 17.5 mg (95%) of a purple powder. **ESI-MS:** (*m*/*z*, pos.): 314.11 ([(^{i}Pr-PNN)$_2$Fe]$^{2+}$ = $C_{34}H_{46}FeN_4P_2^{2+}$). **^{1}H NMR** (400 MHz, CD_3OD, 23 °C): δ = 0.37 (dd, 3 H, $^3J_{PH}$ = 14.0 Hz, $^3J_{HH}$ = 7.2 Hz, ^{i}Pr−CH_3^A), 0.73 (dd, 3 H, $^3J_{PH}$ = 15.3 Hz, $^3J_{HH}$ = 7.3 Hz, ^{i}Pr−CH_3'^{A}), 0.82 (dd, 3 H, $^3J_{PH}$ = 12.1 Hz, $^3J_{HH}$ = 7.0 Hz, ^{i}Pr−CH_3^B), 1.45 (dd, 3 H, $^3J_{PH}$ = 10.6 Hz, $^3J_{HH}$ = 7.0 Hz, ^{i}Pr−CH_3'^{B}), 2.09 (m, 1 H, ^{i}Pr−C*H*), 2.45 (m, 1 H, ^{i}Pr−C*H*′), 3.30 (s, br, 2H, PCH_2), 7.33 (vt, (dd), 1 H, $^3J_{HH}$ = 5.7 Hz, *H*12), 7.36 (d, 1 H, $^3J_{HH}$ = 5.1 Hz, *H*13), 8.00 (m, (d+t), 2 H, *H*5 + 11), 8.23 (vt, 1 H, $^3J_{HH}$ = 7.7 Hz, *H*6), 8.52 (d, 1 H, $^3J_{HH}$ = 7.9 Hz, *H*10), 8.66 (d, 1 H, $^3J_{HH}$ = 7.8 Hz, *H*7) ppm. **^{1}H{^{31}P} NMR** (400 MHz, CD_3OD, 23 °C): δ = 0.37 (d, 3 H, $^3J_{HH}$ = 7.2 Hz, ^{i}Pr−CH_3^A), 0.73 (d, 3 H, $^3J_{HH}$ = 7.3 Hz, ^{i}Pr−CH_3'^{A}), 0.82 (d, 3 H, $^3J_{HH}$ = 7.1 Hz, ^{i}Pr−CH_3^B), 1.45 (d, 3 H, $^3J_{HH}$ = 7.0 Hz, ^{i}Pr−CH_3'^{B}),

dx.doi.org/10.1021/ic401432m | *Inorg. Chem.* 2013, 52, 9636−9649

2.09 (sept, 2 H, $^3J_{HH}$ = 7.0 Hz, ^{i}Pr−C*H*), 2.45 (sept, 2 H, $^3J_{HH}$ = 7.1 Hz, ^{i}Pr−C*H*′), 3.30 (s, br, 2H, PCH_2), 7.33 (vt, (dd), 1 H, $^3J_{HH}$ = 5.8 Hz, *H*12), 7.36 (d, 1 H, $^3J_{HH}$ = 5.1 Hz, *H*13), 8.00 (m, (d+t) 2 H, *H*5 + 11), 8.23 (vt, 1 H, $^3J_{HH}$ = 7.8 Hz, *H*6), 8.52 (d, 1 H, $^3J_{HH}$ = 7.9 Hz, *H*10), 8.66 (d, 1 H, $^3J_{HH}$ = 7.9 Hz, *H*7) ppm. **^{13}C{^{1}H} NMR** (100 MHz, CD_3OD, 23 °C): δ = 19.0 (br, ^{i}Pr-CH_3^A), 19.5 (vt, (dd), J_{PH} = 1.5 Hz, ^{i}Pr-$CH_3^{'A}$), 19.6 (vt, (dd), J_{PH} = 4.5 Hz, ^{i}Pr-$CH_3^{'B}$), 19.8 (vt, (dd), J_{PH} = 4.5 Hz, ^{i}Pr-CH_3^B), 27.0 (vt, (dd), J_{PH} = 9.0 Hz, ^{i}Pr-CH), 31.6 (vt, (dd), J_{PH} = 7.7 Hz, ^{i}Pr-CH), 49.3 (vt, (dd), J_{PH} = 21.4 Hz, CH_2P), 124.1 (s, *C*6), 125.0 (s, *C*10), 126.0 (vt, (dd), J_{PC} = 4.0 Hz, *C*5), 128.7 (s, *C*12), 139.0 (s, *C*6), 140.0 (s, *C*11), 151.5 (s, *C*13), 159.7 (s, br, *C*9), 160.4 (vt, (dd), J_{PC} = 1.7 Hz, *C*8), 168.0 (vt, (dd), J_{PC} = 3.0 Hz, *C*4) ppm. **^{31}P{^{1}H} NMR** (121 MHz, CD_3OD, 23 °C): δ = 60.6 (s) ppm. **Magnetic susceptibility** (Evans): no paramagnetic shifting of the reference could be observed (benzene in CD_3OD, 23 °C).

*[(^{i}Pr-PNN)$_2$Fe](Br)$_2$ (**6**).* A solution of ^{i}Pr-PNN (21.0 mg, 73.3 μmol) in 1 mL of THF was added to a solution of $FeBr_2$ (5.0 mg, 23.4 μmol) in 4 mL of THF. Upon addition a black suspension was formed. Pentane (15 mL) was added to the purple suspension after 72 h of stirring at room temperature. The suspension was filtered, the residue was washed with pentane (20 mL), and dried in vacuo to yield 17.5 mg (95%) of a purple powder. Single crystals of **6** were obtained by slow diffusion of diethylether into a saturated solution of the complex in acetonitrile. **Anal. Calcd. (found)** for $C_{34}H_{46}Br_2FeN_4P_2$ [788.36 g·mol^{-1}]: C 51.80 (52.07), H 5.88 (5.75), N 7.11 (7.09). **ESI-MS:** (*m*/*z*, pos.): 314.11 ([(^{i}Pr-PNN)$_2$Fe]$^{2+}$ = $C_{34}H_{46}FeN_4P_2^{2+}$); (*m*/*z*, neg.): 78.94 (Br^-). ^{1}H, ^{13}C{^{1}H}, and ^{31}P{^{1}H} NMR spectra are identical to the chloro complex **5**. **^{15}N NMR** (41 MHz, CD_3OD, 23 °C): δ = 254.7 (N1), 260.7 (N2) ppm. **Magnetic susceptibility** (Evans): no paramagnetic shifting of the reference could be observed (benzene in CD_3OD, 23 °C).

*[(Ph-PNN)$_2$Fe](FeCl$_4$) (**7**).* Ph-PNN (72.0 mg, 0.203 mmol) was added to a suspension of $FeCl_2$ (25.2 mg, 0.200 mmol) in 12 mL of THF. Upon addition the reaction mixture turned red. After 16 h of stirring at room temperature, the volume of the resulting suspension was reduced in vacuo to about 5 mL, and pentane (15 mL) was added. The suspension was filtered, the residue was washed with pentane (20 mL) and dried in vacuo to yield 88.5 mg (93%) of an orange colored powder. **Anal. Calcd. (found)** for $C_{46}H_{38}Cl_4Fe_2N_4P_2$ [960.00 g·mol^{-1}]: C 57.42 (57.23), H 3.98 (4.04), N 5.82 (5.72). **ESI-MS**: (*m*/*z*, pos.): 799.18 ([(Ph-PNN)$_2$Fe(Cl)]$^+$ = $C_{46}H_{38}ClFeN_4P_2^+$), 445.11 ([(Ph-PNN)Fe(Cl)]$^+$ = $C_{26}H_{19}ClFeN_2P^+$), 382.02 ([(Ph-PNN)$_2$Fe]$^{2+}$ = $C_{46}H_{38}FeN_4P_2^{2+}$); (*m*/*z*, neg.): 160.84 ($FeCl_3^-$). **^{1}H NMR** (400 MHz, CD_3OD, 23 °C): δ = 4.04 (dd, 1 H, $^2J_{HH}$ = 17.5 Hz, $^2J_{PH}$ = 8.1 Hz, Ph_2PCHH), 4.91 (m, 1 H, Ph_2PCHH), 6.60 (m, 1 H, *H*15), 6.74 (m, 2 H, *H*3′), 6.74 (m, 1 H, *H*14), 6.80 (m, 2 H, *H*3), 6.92 (vt, 2 H, $^3J_{HH}$ = 7.4 Hz, *H*2), 7.03 (t, 1 H, $^3J_{HH}$ = 7.4 Hz, *H*1), 7.21 (vt, 2 H, $^3J_{HH}$ = 7.4 Hz, *H*2′), 7.42 (t, 1 H, $^3J_{HH}$ = 7.4 Hz, *H*1′), 7.64 (vt, 1 H, $^3J_{HH}$ = 7.4 Hz, *H*13), 8.26 (d, 1 H, $^3J_{HH}$ = 8.1 Hz, *H*12), 8.29 (d, 1 H, $^3J_{HH}$ = 8.0 Hz, *H*7), 8.40 (vt, 1 H, $^3J_{HH}$ = 8.0 Hz, *H*8), 8.66 (d, 1 H, $^3J_{HH}$ = 8.0 Hz, *H*9) ppm. **^{1}H{^{31}P} NMR** (400 MHz, CD_3OD, 23 °C): δ = 4.02 (d, 1 H, $^2J_{HH}$ = 18.1 Hz, Ph_2PCHH), 4.91 (d, 1 H, $^2J_{HH}$ = 18.2 Hz, Ph_2PCHH), 6.59 (d, br, 1 H, $^2J_{HH}$ = 5.1 Hz, *H*15), 6.74 (m, 2 H, *H*3′), 6.74 (m, 1 H, *H*14), 6.78 (d, 2 H, $^3J_{HH}$ = 7.7 Hz, *H*3), 6.90 (vt, 2 H, $^3J_{HH}$ = 7.4 Hz, *H*2), 7.02 (t, 1 H, $^3J_{HH}$ = 7.4 Hz, *H*1), 7.20 (vt, 2 H, $^3J_{HH}$ = 7.4 Hz, *H*2′), 7.41 (t, 1 H, $^3J_{HH}$ = 7.4 Hz, *H*1′), 7.64 (vt, 1 H, $^3J_{HH}$ = 7.4 Hz, *H*13), 8.26 (d, 1 H, $^3J_{HH}$ = 8.1 Hz, *H*12), 8.29 (d, 1 H, $^3J_{HH}$ = 8.0 Hz, *H*7), 8.40 (vt, 1 H, $^3J_{HH}$ = 8.0 Hz, *H*8), 8.66 (d, 1 H, $^3J_{HH}$ = 8.0 Hz, *H*9) ppm. **^{13}C{^{1}H} NMR** (100 MHz, CD_3OD, 23 °C): δ = 37.4 (m, br, CH_2PPh_2), 124.1 (s, *C*9), 124.6 (s, *C*12), 126.2 (m, *C*7), 128.3 (s, *C*3′), 130.0 (m, *C*2′), 130.4 (m, *C*3), 130.5 (m, *C*2′) 130.8 (s, *C*1), 131.4 (m, *C*14), 131.4 (d, $^2J_{CP}$= 38.5 Hz, *C*4′), 131.7 (d, $^2J_{CP}$= 39.6 Hz, *C*4), 132.2 (s, *C*1′), 139.0 (s, *C*13), 139.9 (s, *C*8), 151.0 (br, *C*15), 157.6 (br, *C*11), 160.2 (m, *C*10), 165.9 (m, *C*6) ppm. **^{31}P{^{1}H} NMR** (162 MHz, C_6D_6, 23 °C): δ = 54.4 (s) ppm. The resonances of H3′and H14 are overlapping in the ^{1}H and ^{1}H{^{31}P} NMR spectra. **Magnetic susceptibility** (Evans): μ_{eff} = 5.1 μ_B (benzene in CD_3OD, 23 °C). This magnetic moment stems from the $FeCl_4^{2-}$ anion (*S* = 2).[26]

*[(Ph-PNN)$_2$Fe](FeBr$_4$) (**8**).* Ph-PNN (72.0 mg, 0.203 mmol) was added to a solution of $FeBr_2$ (43.0 mg, 0.201 mmol) in 10 mL of THF. Upon addition the reaction mixture turned red. After 16 h of stirring at room temperature pentane (10 mL) was added. The suspension was filtered, and the residue was washed with pentane (20 mL) and dried in vacuo to yield 110.1 mg (97%) of an orange colored powder. Single crystals of **6** suitable for X-ray analysis were obtained by slow diffusion of Et_2O into a saturated solution of the complex in acetonitrile. **Anal. Calcd. (found)** for $C_{46}H_{38}Br_4Fe_2N_4P_2$ [1135.80 g·mol^{-1}]: C 48.46 (48.76), H 3.36 (3.42), N 4.91 (4.64). **ESI-MS**: (*m*/*z*, pos.): 845.13 ([(Ph-PNN)$_2$Fe(Br)]$^+$ = $C_{46}H_{38}BrFeN_4P_2^+$), 382.02 ([(Ph-PNN)$_2$Fe]$^{2+}$ = $C_{46}H_{38}FeN_4P_2^{2+}$); (*m*/*z*, neg.): 294.07 ($FeBr_3^-$), 80.97 (Br^-). ^{1}H, ^{13}C{^{1}H}, and ^{31}P{^{1}H} NMR spectra are identical to the chloro complex **7**. **^{15}N NMR** (41 MHz, CD_3OD, 23 °C): δ = 254.9 (N2), 256.7 (N1) ppm. **Magnetic susceptibility** (Evans): μ_{eff} = 5.1 μ_B (benzene in CD_3OD, 23 °C). This magnetic moment stems from the $FeBr_4^{2-}$ anion (*S* = 2).[26]

[(^{i}Pr-PNN)$_2$Fe] (**9**).* Complex **6** (32.0 mg, 40.7 μmol) and KO^{t}Bu (11.2 mg, 0.10 mmol) were suspended in THF (10 mL), and the reaction mixture was stirred at room temperature for 8 h. All volatiles were removed in vacuo, and 20 mL of a 1:2 mixture of toluene and benzene was added. The resulting suspension was filtered, and all volatiles were removed in vacuo to obtain 23.0 mg (90%) of a dark brown solid. **^{1}H NMR** (500 MHz, C_6D_6, 23 °C): δ = 0.60 (dd, 3 H, $^3J_{PH}$ = 12.3 Hz, $^3J_{HH}$ = 7.2 Hz, ^{i}Pr−CH_3^A), 0.90 (m, 3 H, ^{i}Pr−CH_3^B), 1.27 (m, 1 H, ^{i}Pr−C*H*), 1.35 (dd, 3 H, $^3J_{PH}$ = 13.7 Hz, $^3J_{HH}$ = 7.3 Hz, ^{i}Pr−$CH_3^{'A}$), 1.43 (dd, 3 H, $^3J_{PH}$ = 10.2 Hz, $^3J_{HH}$ = 7.5 Hz, ^{i}Pr−$CH_3^{'B}$), 2.89 (m, 1 H, ^{i}Pr−C*H*′), 4.03 (s, br, 1 H, *H*3), 5.99 (vt, br, 1 H, $^3J_{HH}$ = 6.7 Hz, *H*12), 6.37 (d, 1 H, $^3J_{HH}$ = 6.3 Hz, *H*7), 6.47 (d, br, 1 H, $^3J_{HH}$ = 8.5 Hz, *H*5), 6.54 (vt, 1 H, $^3J_{HH}$ = 8.1 Hz, *H*11), 6.78 (vt, 1 H, $^3J_{HH}$ = 7.7 Hz, *H*6), 7.01 (d, br, 1 H, $^3J_{HH}$ = 8.0 Hz, *H*10), 7.81 (d, br, 1 H, $^3J_{HH}$ = 5.2 Hz, *H*13) ppm. **^{1}H{^{31}P} NMR** (500 MHz, C_6D_6, 23 °C): δ = 0.60 (d, 3 H, $^3J_{HH}$ = 7.2 Hz, ^{i}Pr−CH_3^A), 0.90 (d, 3 H, $^3J_{HH}$ = 7.3 Hz, ^{i}Pr−CH_3^B), 1.27 (m, 1 H, ^{i}Pr−C*H*), 1.35 (d, 3 H, $^3J_{HH}$ = 7.2 Hz, ^{i}Pr−$CH_3^{'A}$), 1.43 (d, 3 H, $^3J_{HH}$ = 7.4 Hz, ^{i}Pr−$CH_3^{'B}$), 2.90 (sept, 1 H, $^3J_{HH}$ = 7.1 Hz, ^{i}Pr−C*H*′), 4.03 (s, br, 1 H, *H*3), 5.99 (vt, br, 1 H, $^3J_{HH}$ = 6.9 Hz, *H*12), 6.37 (d, 1 H, $^3J_{HH}$ = 6.5 Hz, *H*7), 6.47 (d, br, 1 H, $^3J_{HH}$ = 8.6 Hz, *H*5), 6.54 (vt, 1 H, $^3J_{HH}$ = 8.2 Hz, *H*11), 6.78 (vt, 1 H, $^3J_{HH}$ = 7.7 Hz, *H*6), 7.01 (d, br, 1 H, $^3J_{HH}$ = 7.6 Hz, *H*10), 7.81 (d, br, 1 H, $^3J_{HH}$ = 5.0 Hz, *H*13) ppm. **^{13}C{^{1}H} NMR** (125 MHz, C_6D_6, 23 °C): δ = 19.9 (m, br, ^{i}Pr-CH_3^B + ^{i}Pr-$CH_3^{'B}$), 20.2 (s, br, ^{i}Pr-CH_3^A), 20.9 (s, br, ^{i}Pr-$CH_3^{'A}$), 29.1 (vt, (dd), J_{PH} = 11.2 Hz, ^{i}Pr-CH′), 31.1 (vt, (dd), J_{PH} = 7.2 Hz, ^{i}Pr-CH′), 67.2 (m, *C*3), 101.2 (s, *C*7), 110.9 (vt, (dd), J_{PH} = 7.1 Hz, *C*5), 119.3 (s, *C*10), 122.7 (s, *C*12), 129.8 (s, *C*6), 132.5 (s, *C*11), 151.1 (s, *C*13), 157.7 (s, *C*8), 162.9 (s, *C*9), 172.1 (vt, (dd), J_{PH} = 9.7 Hz, *C*4) ppm. **^{31}P{^{1}H} NMR** (202 MHz, C_6D_6, 23 °C): δ = 51.8 (s) ppm. **^{15}N NMR** (41 MHz, C_6D_6, 23 °C): δ = 199.7 (N2), 273.2 (N1) ppm. **Magnetic susceptibility** (Evans): no paramagnetic shifting of the reference could be observed (dioxane in C_6D_6, 23 °C).

[(Ph-PNN)$_2$Fe] (**10**).* Complex **8** (34.8 mg, 30.6 μmol) and KO^{t}Bu (7.9 mg, 70.4 μmol) were suspended in THF (10 mL), and the reaction mixture was stirred at room temperature for 8 h. All volatiles were removed in vacuo, and 20 mL of a 1:2 mixture of toluene and benzene was added. The resulting suspension was filtered, and all volatiles were removed in vacuo to obtain 20.4 mg (87%) of a dark brown solid. **^{1}H NMR** (500 MHz, C_6D_6, 23 °C): δ = 4.43 (s, br, 1 H, Ph_2PCH), 5.80 (t, 1 H, $^2J_{HH}$ = 6.3 Hz, *H*14), 6.27 (t, 1 H, $^2J_{HH}$ = 7.3 Hz, *H*13), 6.35 (d, 1 H, $^2J_{HH}$ = 7.0 Hz, *H*9), 6.56 (d, 1 H, $^2J_{HH}$ = 8.0 Hz, *H*12), 6.60 (m, br, 3 H, *H*1′+H2′), 6.77 (m, 1 H, *H*1), 6.84 (t, 2 H, $^2J_{HH}$ = 7.3 Hz, *H*2′), 6.93 (d, br, 1 H, $^2J_{HH}$ = 8.5 Hz, *H*7), 7.04 (t, 1 H, $^2J_{HH}$ = 7.8 Hz, *H*8), 7.25 (br, 2 H, *H*3′), 7.62 (d, br, 1 H, $^2J_{HH}$ = 5.3 Hz, *H*15), 7.68 (br, 2 H, *H*3) ppm. **^{1}H{^{31}P} NMR** (500 MHz, C_6D_6, 23 °C): δ = 4.43 (s, br, 1 H, Ph_2PCH), 5.80 (t, 1 H, $^2J_{HH}$ = 6.3 Hz, *H*14), 6.27 (t, 1 H, $^2J_{HH}$ = 7.3 Hz, *H*13), 6.35 (d, 1 H, $^2J_{HH}$ = 6.9 Hz, *H*9), 6.57 (d, 1 H, $^2J_{HH}$ = 7.8 Hz, *H*12), 6.60 (m, br, 3 H, *H*1′+H2′), 6.77 (m, 1 H, *H*1), 6.85 (t, 2 H, $^2J_{HH}$ = 7.3 Hz, *H*2′), 6.94 (d, 1 H, $^2J_{HH}$ = 8.5 Hz, *H*7), 7.05 (t, 1 H, $^2J_{HH}$ = 7.8 Hz, *H*8), 7.26 (d, 2 H, $^2J_{HH}$ = 7.6 Hz, *H*3′), 7.62 (d, br, 1 H, $^2J_{HH}$ = 5.3 Hz, *H*15), 7.65 (d, br, 2 H, $^2J_{HH}$ = 7.3 Hz, *H*3) ppm. **^{13}C{^{1}H} NMR** (100 MHz, CD_3OD, 23 °C): δ = 60.7 (m, $CHPPh_2$), 101.8 (s, *C*9), 124.6 (s, *C*12), 111.6 (vt, $^3J_{CP}$ = 8.2 Hz, *C*7), 119.6 (s, *C*12), 122.9 (s, *C*14), 126.1 (s, *C*1′), 127.0 (vt, $^3J_{CP}$ = 4.2 Hz, *C*2′), 127.2 (vt, $^3J_{CP}$ = 4.6 Hz, *C*2), 127.3 (s, *C*1), 130.5 (vt, $^2J_{CP}$ = 4.3 Hz, *C*3′), 131.0 (s, *C*8), 131.8 (vt, $^2J_{CP}$= 4.4

dx.doi.org/10.1021/ic401432m | *Inorg. Chem.* 2013, 52, 9636−9649

Hz, *C*3), 132.4 (s, *C*13), 138.9 (m, *C*4′), 139.5 (m, *C*4), 150.8 (s, *C*15), 157.3 (vt, $^3J_{CP}$ = 2.2 Hz, *C*10), 161.0 (s, *C*11), 173.9 (vt, $^2J_{CP}$ = 11.7 Hz, *C*6) ppm. **^{31}P{^{1}H} NMR** (162 MHz, C_6D_6, 23 °C): δ = 50.6 (s) ppm. **^{15}N NMR** (41 MHz, toluene-d_8, 23 °C): δ = 204.7 (N2), 269.5 (N1) ppm. The resonances of H1′and H2′ are overlapping in the ^{1}H and ^{1}H{^{31}P} NMR spectra. **Magnetic susceptibility** (Evans): no paramagnetic shifting of the reference could be observed (dioxane in C_6D_6, 23 °C).

*[(Ph-PNN)$_2$Fe](PF$_6$)$_2$ (**11**).* Complex **8** (98.0 mg, 86.2 μmol) and TlPF$_6$ (136.0 mg, 0.39 mmol) were suspended in DCM (20 mL), and the reaction mixture was stirred at room temperature for 48 h. The insoluble precipitate was filtered off and washed with DCM (2 × 10 mL). The solutions were combined, and all volatiles were removed in vacuo to obtain 52.4 mg (58%) of an orange colored solid. **^{1}H NMR** (400 MHz, CD_3CN, 23 °C): δ = 4.01 (dvt, 1 H, $^2J_{HH}$ = 18.0 Hz, J_{PH} = 4.4 Hz, Ph_2PCH*H*), 4.76 (dvt, 1 H, $^2J_{HH}$ = 18.1 Hz, J_{PH} = 7.0 Hz, Ph_2PCH*H*), 6.54 (d, br, 1 H, $^3J_{HH}$ = 5.5 Hz, *H*14), 6.71 (m, 2 H, *H*3′), 6.71 (m, 1 H, *H*14), 6.77 (m, 2 H, *H*3), 6.93 (vt, 2 H, $^3J_{HH}$ = 7.4 Hz, *H*2), 7.07 (t, 1 H, $^3J_{HH}$ = 7.4 Hz, *H*1), 7.22 (vt, 2 H, $^3J_{HH}$ = 7.4 Hz, *H*2′), 7.45 (t, 1 H, $^3J_{HH}$ = 7.4 Hz, *H*1′), 7.61 (vt, 1 H, $^3J_{HH}$ = 8.2 Hz, *H*13), 8.08 (d, 1 H, $^3J_{HH}$ = 8.0 Hz, *H*12), 8.19 (d, 1 H, $^3J_{HH}$ = 7.8 Hz, *H*7), 8.36 (vt, 1 H, $^3J_{HH}$ = 7.9 Hz, *H*8), 8.48 (d, 1 H, $^3J_{HH}$ = 8.0 Hz, *H*9) ppm. **^{1}H{^{31}P} NMR** (400 MHz, CD_3CN, 23 °C): δ = 4.01 (d, 1 H, $^2J_{HH}$ = 18.2 Hz), 4.76 (d, 1 H, $^2J_{HH}$ = 18.2 Hz), 6.54 (d, br, 1 H, $^3J_{HH}$ = 5.3 Hz, *H*14), 6.71 (m, 2 H, *H*3′), 6.71 (m, 1 H, *H*14), 6.77 (m, 2 H, *H*3), 6.93 (vt, 2 H, $^3J_{HH}$ = 7.8 Hz, *H*2), 7.07 (t, 1 H, $^3J_{HH}$ = 7.5 Hz, *H*1), 7.22 (vt, 2 H, $^3J_{HH}$ = 7.8 Hz, *H*2′), 7.45 (t, 1 H, $^3J_{HH}$ = 7.5 Hz, *H*1′), 7.61 (vt, 1 H, $^3J_{HH}$ = 7.8 Hz, *H*13), 8.08 (d, 1 H, $^3J_{HH}$ = 8.0 Hz, *H*12), 8.19 (d, 1 H, $^3J_{HH}$ = 7.8 Hz, *H*7), 8.36 (vt, 1 H, $^3J_{HH}$ = 7.9 Hz, *H*8), 8.47 (d, 1 H, $^3J_{HH}$ = 8.0 Hz, *H*9) ppm. **^{31}P{^{1}H} NMR** (162 MHz, CD_3CN, 23 °C): δ = −143.4 (sept, $^1J_{PF}$ = 706.6 Hz, PF_6^-), 54.2 (s, Ph-*P*NN) ppm. **^{19}F{^{1}H} NMR** (377 MHz, CD_3CN, 23 °C): δ = −73.6 (sept, $^1J_{PF}$ = 706.9 Hz, PF_6^-) ppm. The resonances of H3′and H14 are overlapping in the ^{1}H and ^{1}H{^{31}P} NMR spectra. **Magnetic susceptibility** (Evans): no paramagnetic shifting of the reference could be observed (dioxane in CD_3CN, 23 °C).

[(Ph-PNN)(Ph-PNN)Fe](PF$_6$) (**12**).* **Route 1.** Complex **10** (7.9 mg, 10.4 μmol) and complex **11** (10.7 mg, 10.2 μmol) were suspended in THF (12 mL), and the reaction mixture was stirred for 36 h at room temperature. All volatiles were removed in vacuo to obtain 18.6 mg (quantitative) of a brownish green solid. **Route 2:** A solution of KO^{t}Bu (10.0 μmol) in CD_3CN (0.6 mL) was added to complex **11** (10.5 mg, 10.0 μmol). Full conversion to complex **12** was observed by NMR spectroscopy. Integration of the benzylic protons as well as the resonances in the ^{31}P{^{1}H} NMR spectrum indicate deuterium incorporation in these positions. A deuteration of about 50% was observed in the protonated as well as the deprotonated benzylic positions after storing the sample for 9 h at room temperature. The asterisk denotes the resonances of the dearomatized pincer ligand. The ^{1}H and ^{1}H{^{31}P}NMR show overlapping resonances. The chemical shifts and the multiplicities of bipyridine resonances that are overlapping with other resonances were determined by 2D NMR experiments (these data is represented in italic). **^{1}H NMR** (500 MHz, CD_3CN, 23 °C): δ = 3.74 (m, 1 H, *H*5), 4.03 (s, br, 1 H, *H*5*), 4.54 (m, 1 H, *H*5′), 6.40 (m, 1 H, *H*14*), 6.46 (m, br, 1 H, *H*15*), 6.67 (m, 5 H, phenyl-*H* + *H*9* *(6.66 ppm, d)*), 6.82 (m, 7 H, phenyl-*H* + *H*7* *(6.84 ppm, d)*), 6.91 (m, 4 H, phenyl-*H* + *H*14 *(6.89 ppm, t)*), 6.98 (vt, 1 H, $^3J_{HH}$ = 7.3 Hz, phenyl-H_{para}), 7.19 (m, 7 H, phenyl-*H* + *H*13* *(7.22 ppm, t)* + *H*8* *(7.14 ppm, t)*), 7.35 (vt, 1 H, phenyl-H_{para}), 7.44 (d, br, 1 H, $^3J_{HH}$ = 8.1 Hz, *H*12*), 7.48 (vt, 1 H, $^3J_{HH}$= 8.4 Hz, *H*13), 7.55 (d, br, 1 H, $^3J_{HH}$= 5.5 Hz, *H*15), 7.94 (d, br, 1 H, $^3J_{HH}$= 8.0 Hz, *H*12), 8.01 (d, br, 1 H, $^3J_{HH}$= 7.7 Hz, *H*7), 8.18 (vt, 1 H, $^3J_{HH}$= 7.9 Hz, *H*8), 8.38 (d, br, $^3J_{HH}$= 7.9 Hz, *H*9) ppm. **^{1}H{^{31}P} NMR** (500 MHz, CD_3CN, 23 °C): δ = 3.74 (d, 1 H, $^2J_{HH}$ = 18.2 Hz, *H*5), 4.03 (s, br, 1 H, *H*5*), 4.56 (m, 1 H, $^2J_{HH}$ = 17.8 Hz, *H*5′), 6.40 (m, 1 H, *H*14*), 6.46 (m, br, 1 H, *H*15*), 6.67 (m, 5 H, phenyl-*H* + *H*9* *(6.66 ppm, d)*), 6.82 (m, 7 H, phenyl-*H* + *H*7* *(6.84 ppm, d)*), 6.91 (m, 4 H, phenyl-*H* + *H*14 *(6.89 ppm, t)*), 6.98 (vt, 1 H, $^3J_{HH}$ = 7.3 Hz, phenyl-H_{para}), 7.19 (m, 7 H, phenyl-*H* + *H*13* *(7.22 ppm, t)* + *H*8* *(7.14 ppm, t)*), 7.35 (vt, 1 H, phenyl-H_{para}), 7.44 (d, br, 1 H, $^3J_{HH}$ = 8.0 Hz, *H*12*), 7.48 (vt, 1 H, $^3J_{HH}$= 7.8 Hz, *H*13), 7.55 (d, br, 1 H, $^3J_{HH}$= 5.6 Hz, *H*15), 7.93 (d, br, 1 H, $^3J_{HH}$= 7.9 Hz, *H*12), 8.01 (d, br, 1 H, $^3J_{HH}$= 7.7 Hz, *H*7), 8.18 (t, 1 H, $^3J_{HH}$= 7.9 Hz, *H*8), 8.38 (d, br, $^3J_{HH}$= 8.0 Hz, *H*9) ppm. **^{13}C{^{1}H} NMR** (125 MHz, CD_3CN, 23 °C): δ = 39.0 (m, CH_2PPh_2), 59.5 (d, $^1J_{CP}$ = 67.8 Hz, CH_2PPh_2), 104.3 (m, *C*9*), 114.9 (m, *C*7*), 121.3 (s, *C*12*),122.9 (s, *C*9), 123.3 (s, *C*12), 124.0 (m, *C*7), 125.6 (s, *C*14*), 126.6 (s, *C*14), 128.2 (d, J_{CP} = 8.7 Hz, phenyl-*C*), 128.4 (d, J_{CP} = 2.2 Hz, phenyl-*C*), 128.6 (d, J_{CP} = 2.2 Hz, phenyl-*C*), 128.6 (d, J_{CP} = 9.2 Hz, phenyl-*C*), 139.1 (d, J_{CP} = 2.2 Hz, phenyl-*C*), 129.2 (m, 2x phenyl-*C*), 130.0 (d, J_{CP} = 8.5 Hz, phenyl-*C*), 130.3 (d, J_{CP} = 8.5 Hz, phenyl-*C*), 131.2 (d, J_{CP} = 2.1 Hz, phenyl-*C*), 131.6 (d, J_{CP} = 9.0 Hz, phenyl-*C*), 132.2 (m, phenyl-C_{ipso}), 132.5 (d, J_{CP} = 9.9 Hz, phenyl-*C*), 133.2 (br, *C*8), 134.5 (m, phenyl-C_{ipso}), 136.3 (s, *C*8), 136.5 (s, *C*13), 136.7 (s, *C*9*), 138.4 (m, 2x phenyl-C_{ipso}), 149.9 (s, *C*15*), 151.7 (s, *C*15), 156.2 (m, *C*10*), 157.9 (s, *C*11), 160.3 (s, *C*11*), 160.9 (m, *C*10) 165.7 (m, *C*6), 174.2 (m, *C*6*) ppm. **^{31}P{^{1}H} NMR** (121 MHz, CD_3CN, 23 °C): δ = −143.4 (sept, $^1J_{PF}$ = 706.4 Hz, PF_6^-), 43.9 (d, $^2J_{PP}$ = 47.6 Hz, Ph-*P*NN*), 61.5 (d, $^2J_{PP}$ = 47.6 Hz, Ph-*P*NN) ppm. **^{19}F{^{1}H} NMR** (377 MHz, CD_3CN, 23 °C): δ = −73.6 (sept, $^1J_{PF}$ = 706.9 Hz, PF_6^-) ppm.

Reactivity Studies of the Complexes 9 and 10. *Reaction of Complex **9** with D$_2$O.* Complex **9** (7.3 mg, 11.7 μmol) was dissolved in D_2O (0.6 mL, 32.7 mmol) under formation of an intense red solution. Full conversion of **9** to [(^{i}Pr-PNN)$_2$Fe]$^{2+}$ was observed according to the ^{1}H and ^{31}P{^{1}H} NMR spectra. The sample did not show any change after 18 h.

*Reaction of Complex **9** with CD$_3$OD.* Complex **9** (5.3 mg, 8.5 μmol) was dissolved in CD_3OD (0.6 mL, 14.8 mmol) under formation of an intense red solution. Full conversion of **9** to [(^{i}Pr-PNN)$_2$Fe]$^{2+}$ was observed according to the ^{1}H and ^{31}P{^{1}H} NMR spectra. The sample did not show any change after 14 h. All volatiles were evaporated, and the sample was exposed to high vacuum for about 6 h resulting in the formation of a brown solid. The solid was extracted with toluene-d_8 (0.6 mL) resulting in a green insoluble residue and a brown solution. ^{1}H and ^{31}P{^{1}H} NMR analysis of the solution shows a mixture of complex **9** with the *mono*-deuterated ligand (^{i}Pr-*P*NN^{HD}) in a ratio of about 1:7. **^{31}P{^{1}H} NMR** (162 MHz, toluene-d_8, 23 °C): δ = 11.2 (vt, $^2J_{PD}$ = 42.2 Hz, ^{i}Pr-*P*NN^{HD}), 51.6 (m, **9^{HD}**) ppm.

*Dissolving **9** in Hexylamine.* Complex **9** (6.7 mg, 10.7 μmol) was dissolved in $HexNH_2$ (0.5 mL, 3.4 mmol) and C_6D_6 (0.1 mL) under formation of an intense brown solution. No protonation of **9** was observed according to the ^{1}H and ^{31}P{^{1}H} NMR spectra. The sample did not show any change after 18 h.

*Exposing **9** to H$_2$ Pressure.* Complex **9** (3.0 mg, 4.8 μmol) was placed in a J. Young NMR tube and dissolved in C_6D_6 (0.6 mL) under formation of an intense brown solution. The NMR tube was pressurized two bars of H_2. No change in color was observed, and the NMR spectra did not indicate any reaction after about 3 h.

*Reaction of Complex **10** with D$_2$O (neat).* D_2O (0.6 mL, 32.7 mmol) was added to complex **10** (5.3 mg, 7.0 μmol) under formation of suspension (orange colored solution, brown precipitate). Further addition of D_2O (1.0 mL, 54.5 mmol) and sonication in an ultrasonic bath did not lead to the formation of a solution. Full conversion of **10** to [(Ph-PNN)$_2$Fe]$^{2+}$ was observed in the ^{1}H and ^{31}P{^{1}H} NMR spectra in the orange colored solution. The sample did not show any change after 16 h.

*Reaction of Complex **10** with D$_2$O (in THF).* Complex **10** (6.8 mg, 8.9 μmol) was dissolved in THF (0.5 mL) to give a brown solution. A ^{31}P{^{1}H} NMR spectrum was recorded, and D_2O (0.4 mL, 21.8 mmol) was added. Upon addition a change in color to intense green was observed. ^{1}H and ^{31}P{^{1}H} NMR measurements showed the formation of [(Ph-PNN)(Ph-PNN*)Fe]$^+$ (by comparison to **12**) and [(Ph-PNN)$_2$Fe]$^{2+}$ (by comparison to **11**) in a ratio of 5.9 to 1.0 (according to integration in the ^{31}P{^{1}H}). The sample did not show any change after 20 h.

*Reaction of Complex **10** with CD$_3$OD.* Complex **10** (5.6 mg, 7.3 μmol) was dissolved in CD_3OD (0.6 mL, 14.8 mmol) forming of an intense redish brown solution. ^{1}H and ^{31}P{^{1}H} NMR measurements showed the formation of [(Ph-PNN)(Ph-PNN*)Fe]$^+$ (by comparison to **12**) and [(Ph-PNN)$_2$Fe]$^{2+}$ (by comparison to **11**) in a ratio of 1:1 (according to integration in the ^{31}P{^{1}H} NMR). The sample did not

dx.doi.org/10.1021/ic401432m | *Inorg. Chem.* 2013, 52, 9636−9649

Table 3. Comparison of the Spin-State Energies (ΔE_e or ΔG_{298}, kcal/mol) for Selected Cases Obtained Using DFT and Multireference Methods

complex	geometry[a]	S	DF-PBE[b]	DSD[c]/SVP[b]	DSD[c]/TZVP[b]	CASSCF[d]	NEVPT2[d]
$[FeCl_4]^{2-}$	triplet (C_{2v})	1	27.4	43.4	41.9	57.8	54.2
		2	0.0	0.0	0.0	0.0	0.0
	quintet (D_2)	1	27.4	43.4	41.9	60.0	57.2
		2	0.0	0.0	0.0	0.0	0.0
complex 3	quintet (C_1)	0	3.3	48.1	42.4	76.0	67.6
		1	0.0	37.4	32.7	50.6	43.0
		2	3.0	0.0	0.0	0.0	0.0

[a]CASSCF and NEVPT2 results are for the geometry optimized for this spin-state; the DFT results used fully optimized geometries for each spin state. [b]Energies are ΔG_{298}. [c]DSD = DSD-PBEP86. [d]Energies are ΔE_e.

Table 4. Crystal Data and Summary of Data Collection and Refinement for 1, 2, 4, 6, 8, and 10[a]

	1	2	4	6	8	10
formula	$C_{19}H_{27}Cl_2FeN_2P$	$C_{19}H_{27}Br_2FeN_2P + C_2H_3N$	$C_{17}H_{23}Br_2FeN_2P$	$C_{34}H_{46}FeN_4P_2 + 2(Br) + C_2H_3N$	$2(C_{46}H_{38}FeN_4P_2) + 2(Br_4Fe) + C_2H_3N$	$C_{46}H_{36}FeN_4P_2 + 1.5(C_6H_6)$
diffractometer	Bruker Apex II	Bruker Apex II	Bruker Apex II	Bruker Apex II	Nonius	Bruker Apex II
crystal description	red prism	orange plate	red chunk	black prism	red plate	black prism
crystal size, [mm^3]	0.28 × 0.20 × 0.20	0.24 × 0.20 × 0.04	0.32 × 0.28 × 0.24	0.22 × 0.17 × 0.07	0.30 × 0.30 × 0.10	0.37 × 0.28 × 0.25
FW, [$g \cdot mol^{-1}$]	441.15	571.12	502.01	829.41	2321.22	879.74
space group	$P2_1/c$	$P\bar{1}$	$P2_1/c$	$P2_1/n$	Cc	$P2_1/c$
crystal system	monoclinic	triclinic	monoclinic	monoclinic	monoclinic	monoclinic
a, [Å]	8.1888(6)	8.6815(3)	8.7592(6)	10.2676(5)	12.674(3)	17.2483(6)
b, [Å]	14.6190(11)	10.2730(4)	14.3618(8)	17.5319(9)	24.218(5)	13.6776(5)
c, [Å]	17.4370(13)	13.7241(5)	15.2256(2)	21.1256(11)	16.214(3)	18.6190(6)
α, [deg]		81.688(2)				
β, [deg]	93.843(4)	87.376(2)	90.642(3)	99.049(3)	108.19(3)	102.225(2)
γ, [deg]		85.020(2)				
cell volume, [$Å^3$]	2082.7(3)	1205.87(8)	1915.2(3)	3755.5(3)	4728.1(19)	4292.9(3)
Z	4	2	4	4	2	4
ρ_{calcd}, [$g \cdot cm^{-3}$]	1.407	1.573	1.741	1.467	1.630	1.361
μ, [mm^{-1}]	1.062	4.017	5.044	2.647	4.099	0.470
no. of reflections	17194	19742	22009	65745	45070	46580
no. of unique reflections	4764	5991	4385	9497	11096	12721
$2\Theta_{max}$, [deg]	54.42	56.76	55.12	57.20	55.16	58.26
R_{int}	0.045	0.021	0.046	0.042	0.068	0.032
no. of parameters (restraints)	232(0)	260(0)	212(0)	424(0)	548(2)	584(0)
final R[b]	0.0385	0.0232	0.0284	0.0368	0.0536	0.0362
final R[c]	0.0584	0.0287	0.0407	0.0483	0.0592	0.0501
GooF	1.023	1.033	1.056	1.144	1.073	1.013

[a]Collected using MoK_α radiation (λ = 0.71073 Å). [b]For data with $I > 2\sigma(I)$. [c]For all data.

show any change in the product ratio after 26 h. All volatiles were evaporated, and the sample was exposed to high vacuum for about 24 h, resulting in the regeneration of complex **10** as a dark brown solid, which was fully soluble in toluene. ^1H NMR analysis of the residue showed that H/D exchange took place, as a result of CD_3OD addition/elimination to the dearomatized complex **10**, resulting in approximately 30% deuteration of complex **10**. **$^{31}P\{^1H\}$ NMR** (162 MHz, toluene-d_8, 23 °C): δ = 50.4 (m, $\mathbf{10^{HD}}$), 50.6 (s, $\mathbf{10^{HH}}$) ppm. The $^{31}P\{^1H\}$ NMR spectrum (see Supporting Information) exhibits two superimposed resonances of $\mathbf{10^{HH}}$ (s) and $\mathbf{10^{HD}}$ (m). The ^2D NMR spectrum shows a broad multiplet of the deuterium atoms in the benzylic position centered at δ = 4.40 ppm (with respect to the natural abundance deuterium resonances of toluene-H_8).

*Dissolving **10** in Hexylamine.* Complex **10** (5.4 mg, 7.1 μmol) was dissolved in $HexNH_2$ (0.5 mL, 3.4 mmol) and C_6D_6 (0.1 mL) under formation of an intense brown solution. No protonation of **10** was observed according to the ^1H and $^{31}P\{^1H\}$ NMR spectra. The sample did not show any change after 18 h.

*Exposing **10** to H_2 Pressure.* Complex **10** (4.1 mg, 5.4 μmol) was placed in a J. Young NMR tube and dissolved in C_6D_6 (0.6 mL) under formation of an intense brown solution. The NMR tube was pressurized with two bars of H_2. No change in color was observed, and the NMR spectra did not indicate any reaction after about 3 h.

*Repeated Reaction of **10** with CD_3OD.* Complex **10** (10.0 mg, 13.1 μmol) was dissolved in CD_3OD (1.0 mL, 24.7 mmol) resulting in the formation of an intense reddish brown solution. The reaction was stirred at room temperature for 15 min, and all volatiles were removed in vacuo resulting in the formation of a brown solid. This procedure was repeated 5 times. The solid was fully soluble in toluene. ^1H NMR analysis of the residue showed approximately 85% deuteration as a result of H/D exchange of **10** with CD_3OD. **$^{31}P\{^1H\}$ NMR** (162 MHz, toluene-d_8, 23 °C): δ = 50.4 (s, br, $\mathbf{10^{DD}}$), 50.4 (m, $\mathbf{10^{HD}}$) ppm. The $^{31}P\{^1H\}$ NMR spectrum (see Supporting Information) exhibits two superimposed resonances of 10^{DD} (s, br) and 10^{HD} (m). The ^2D NMR spectrum show a broad resonance of the deuterium atoms in the benzylic position centered at δ = 4.35 ppm (with respect to the natural abundance deuterium resonances of the toluene-H_8).

dx.doi.org/10.1021/ic401432m | Inorg. Chem. 2013, 52, 9636−9649

Computational Details. All DFT calculations were carried out using Gaussian 09 Revision C.01.[31] Two DFT functionals were used. Geometries were optimized and vibrational frequencies were calculated using the Perdew–Burke–Ernzerhof (PBE) GGA functional.[32] Accurate energies were calculated using one of the latest double–hybrid functionals by Kozuch and Martin: DSD–PBEP86.[33] This double–hybrid functional incorporates the PBE[34] DFT exchange functional with "exact" Hartree–Fock exchange, the Perdew-86 (P86) correlation functional[35] with "exact" spin–component scaled[36] second-order Møller–Plesset[37] (SCS–MP2) correlation, and an empirical dispersion correction,[38] specifically Grimme's third version of his empirical dispersion correction (DFTD3)[38a,39] with Becke–Johnson (BJ) dampening.[39,40]

With these two functionals, the split-valence (double-ζ quality) and the triple-ζ basis sets, each with added polarization functions (i.e., the SVP and TZVP basis sets, respectively) of Ahlrichs and co-workers were used.[41] The SVP basis set was used for geometry optimizations while energies were calculated using the TZVP basis set.

To improve the efficiency of the calculations, density-fitting basis sets (DFBS) were employed during the calculation of the Coulomb interaction;[42] this is indicated by appending "DF-" to the functional name. The SVPFit density fitting basis set,[43] specifically designed for SVP, was used.

The accuracy of the DFT method was improved by adding the second generation empirical dispersion correction recommended by Grimme.[44] The older version (DFTD2)[38c] is available, with analytical gradients and Hessians, in Gaussian09 and was used during geometry optimizations and frequency calculations. As noted above, DSD–PBEP86 includes, *per definition*, a DFTD3 correction with BJ–scaling in its functional form, which was calculated using a program written by Grimme.[38a]

Bulk solvent effects were approximated by single point energy calculations using a polarizable continuum model (PCM),[45] specifically the integral equation formalism model (IEF-PCM)[45a,b,46] with the same solvents as in the experiments. Specifically, Truhlar and co-workers' Solvation Model with Dispersion (SMD) was used.[47]

Geometries were optimized using the default pruned (75,302) grid, while the "ultrafine" (i.e., a pruned (99,590)) grid was used for energy and solvation calculations.

To evaluate the accuracy of the double-hybrid functional to predict the correct ground spin-state of the iron complexes, these results were compared, for two selected cases, to results from multireference methods. Complete active space self-consistent field (CASSCF)[48] and *n*-electron valence state perturbation theory (NEVPT2)[49] calculations were performed using Orca version 2.9.0[50] using the DF-PBE optimized geometries. Singlet, triplet, and quintet states were considered as was symmetry. The active space was determined based on a natural orbital analysis as recommended in the Orca Users' Manual. Thus, an active space of 10 electrons in 8 molecular orbitals (i.e., CASSCF(10,8)) was selected. The efficiency of the calculation was improved by using the resolution of identity–chain of spheres (RIJCOSX) approximation.[51] Table 3 compares the DF-PBE, DSD-PBEP86, CASSCF, and NEVPT2 results; while DF-PBE is clearly not suitable, the double hybrid functional predicts the correct spin state but with energies differences smaller than for the multireference methods.

X-ray Structure Determinations. Crystal data and summary of data collection and refinement for complexes **1**, **2**, **4**, **6**, **8**, and **10** are given in Table 4.

■ ASSOCIATED CONTENT

Supporting Information

X-ray crystallographic data for the complexes **1**, **2**, **4**, **6**, **8**, and **10** in cif format, spectroscopic details, and Cartesian (x, y, z) coordinates of all DFT optimized structures. This material is available free of charge via the Internet at http://pubs.acs.org.

■ AUTHOR INFORMATION

Corresponding Author

*E-mail: david.milstein@weizmann.ac.il.

Author Contributions

The manuscript was written through contributions of all authors. All authors have given approval to the final version of the manuscript.

Notes

The authors declare no competing financial interest.

■ ACKNOWLEDGMENTS

This research was supported by the European Research Council under the FP7 framework (ERC No. 246837) and by the Kimmel Center for Molecular Design. T.Z. received a Postdoctoral Fellowship from the MINERVA Foundation, and R.L. received a postdoctoral fellowship from the Deutsche Forschungsgemeinschaft (DFG). D.M. holds the Israel Matz Professorial Chair of Organic Chemistry.

■ DEDICATION

This paper is dedicated to Prof. Dr. Werner Uhl on the occasion of his 60th birthday.

■ REFERENCES

(1) (a) Small, B. L.; Brookhart, M. *J. Am. Chem. Soc.* **1998**, *120*, 7143–7144. (b) Small, B. L.; Brookhart, M.; Bennett, A. M. A. *J. Am. Chem. Soc.* **1998**, *120*, 4049–4050.

(2) (a) Britovsek, G. J. P.; Gibson, V. C.; McTavish, S. J.; Solan, G. A.; White, A. J. P.; Williams, D. J.; Britovsek, G. J. P.; Kimberley, B. S.; Maddox, P. J. *Chem. Commun.* **1998**, 849–850. (b) Britovsek, G. J. P.; Bruce, M.; Gibson, V. C.; Kimberley, B. S.; Maddox, P. J.; Mastroianni, S.; McTavish, S. J.; Redshaw, C.; Solan, G. A.; Strömberg, S.; White, A. J. P.; Williams, D. J. *J. Am. Chem. Soc.* **1999**, *121*, 8728–8740.

(3) (a) Ittel, S. D.; Johnson, L. K.; Brookhart, M. *Chem. Rev.* **2000**, *100*, 1169–1204. (b) Gibson, V. C.; Spitzmesser, S. K. *Chem. Rev.* **2003**, *103*, 283–316. (c) Bianchini, C.; Giambastiani, G.; Rios, I. G.; Mantovani, G.; Meli, A.; Segarra, A. M. *Coord. Chem. Rev.* **2006**, *250*, 1391–1418. (d) Gibson, V. C.; Redshaw, C.; Solan, G. A. *Chem. Rev.* **2007**, *107*, 1745–1776. (e) Gibson, V.; Solan, G. Iron-Based and Cobalt-Based Olefin Polymerisation Catalysts. In *Topics in Organmetallic Chemistry*; Guan, Z., Ed.; Springer: Berlin, Germany, 2009; Vol. *26*, pp 107–158; (f) Bianchini, C.; Giambastiani, G.; Luconi, L.; Meli, A. *Coord. Chem. Rev.* **2010**, *254*, 431–455. (g) Jie, S.-Y.; Sun, W.-H.; Xiao, T. *Chin. J. Polym. Sci.* **2010**, *28*, 299–304. (h) Bhattacharya, P.; Guan, H. *Comments Inorg. Chem.* **2011**, *32*, 88–112.

(4) (a) Bart, S. C.; Lobkovsky, E.; Chirik, P. J. *J. Am. Chem. Soc.* **2004**, *126*, 13794–13807. (b) Bart, S. C.; Lobkovsky, E.; Bill, E.; Chirik, P. J. *J. Am. Chem. Soc.* **2006**, *128*, 5302–5303. (c) Trovitch, R. J.; Lobkovsky, E.; Bill, E.; Chirik, P. J. *Organometallics* **2008**, *27*, 1470–1478. (d) Russell, S. K.; Darmon, J. M.; Lobkovsky, E.; Chirik, P. J. *Inorg. Chem.* **2010**, *49*, 2782–2792.

(5) (a) Tondreau, A. M.; Lobkovsky, E.; Chirik, P. J. *Org. Lett.* **2008**, *10*, 2789–2792. (b) Tondreau, A. M.; Darmon, J. M.; Wile, B. M.; Floyd, S. K.; Lobkovsky, E.; Chirik, P. J. *Organometallics* **2009**, *28*, 3928–3940. (c) Russell, S. K.; Milsmann, C.; Lobkovsky, E.; Weyhermüller, T.; Chirik, P. J. *Inorg. Chem.* **2011**, *50*, 3159–3169. (d) Tondreau, A. M.; Atienza, C. C. H.; Darmon, J. M.; Milsmann, C.; Hoyt, H. M.; Weller, K. J.; Nye, S. A.; Lewis, K. M.; Boyer, J.; Delis, J. G. P.; Lobkovsky, E.; Chirik, P. J. *Organometallics* **2012**, *31*, 4886–4893. (e) Tondreau, A. M.; Atienza, C. C. H.; Weller, K. J.; Nye, S. A.; Lewis, K. M.; Delis, J. G. P.; Chirik, P. J. *Science* **2012**, *335*, 567–570.

(6) (a) Danopoulos, A. A.; Wright, J. A.; Motherwell, W. B. *Chem. Commun.* **2005**, 784–786. (b) Bartholomew, E. R.; Volpe, E. C.; Wolczanski, P. T.; Lobkovsky, E. B.; Cundari, T. R. *J. Am. Chem. Soc.* **2013**, *135*, 3511–27.

(7) (a) Pugh, D.; Wells, N. J.; Evans, D. J.; Danopoulos, A. A. *Dalton Trans.* **2009**, 7189–7195. (b) Trovitch, R. J.; Lobkovsky, E.; Chirik, P. J. *Inorg. Chem.* **2006**, *45*, 7252–7260. (c) Danopoulos, A. A.; Pugh, D.; Smith, H.; Saßmannshausen, J. *Chem.—Eur. J.* **2009**, *15*, 5491–5502.

(d) Darmon, J. M.; Stieber, S. C. E.; Sylvester, K. T.; Fernández, I.; Lobkovsky, E.; Semproni, S. P.; Bill, E.; Wieghardt, K.; DeBeer, S.; Chirik, P. J. *J. Am. Chem. Soc.* **2012**, *134*, 17125−17137.
(8) (a) Benito-Garagorri, D.; Puchberger, M.; Mereiter, K.; Kirchner, K. *Angew. Chem., Int. Ed.* **2008**, *47*, 9142−9145. (b) Benito-Garagorri, D.; Alves, L. G. a.; Puchberger, M.; Mereiter, K.; Veiros, L. F.; Calhorda, M. J.; Carvalho, M. D.; Ferreira, L. P.; Godinho, M.; Kirchner, K. *Organometallics* **2009**, *28*, 6902−6914. (c) Benito-Garagorri, D.; Alves, L. G. a.; Veiros, L. F.; Standfest-Hauser, C. M.; Tanaka, S.; Mereiter, K.; Kirchner, K. *Organometallics* **2010**, *29*, 4932−4942. (d) Benito-Garagorri, D.; Lagoja, I.; Veiros, L. F.; Kirchner, K. A. *Dalton Trans.* **2011**, *40*, 4778−4792.
(9) Langer, R.; Leitus, G.; Ben-David, Y.; Milstein, D. *Angew. Chem., Int. Ed.* **2011**, *50*, 2120−2124.
(10) Langer, R.; Iron, M. A.; Konstantinovski, L.; Diskin-Posner, Y.; Leitus, G.; Ben-David, Y.; Milstein, D. *Chem.—Eur. J.* **2012**, *18*, 7196−209.
(11) Langer, R.; Diskin-Posner, Y.; Leitus, G.; Shimon, L. J. W.; Ben-David, Y.; Milstein, D. *Angew. Chem., Int. Ed.* **2011**, *50*, 9948−9952.
(12) Zell, T.; Butschke, B.; Ben-David, Y.; Milstein, D. *Chem.—Eur. J.* **2013**, *19*, 8068−8072.
(13) Balaraman, E.; Gnanaprakasam, B.; Shimon, L. J. W.; Milstein, D. *J. Am. Chem. Soc.* **2010**, *132*, 16756−16758.
(14) Balaraman, E.; Ben-David, Y.; Milstein, D. *Angew. Chem., Int. Ed.* **2011**, *50*, 11702−11705.
(15) Balaraman, E.; Gunanathan, C.; Zhang, J.; Shimon, L. J. W.; Milstein, D. *Nat. Chem.* **2011**, *3*, 609−614.
(16) Balaraman, E.; Fogler, E.; Milstein, D. *Chem. Commun.* **2012**, *48*, 1111−1113.
(17) Srimani, D.; Feller, M.; Ben-David, Y.; Milstein, D. *Chem. Commun.* **2012**, *48*, 11853−11855.
(18) Srimani, D.; Balaraman, E.; Gnanaprakasam, B.; Ben-David, Y.; Milstein, D. *Adv. Synth. Catal.* **2012**, *354*, 2403−2406.
(19) Balaraman, E.; Khaskin, E.; Leitus, G.; Milstein, D. *Nat. Chem.* **2013**, *5*, 122−125.
(20) Srimani, D.; Ben-David, Y.; Milstein, D. *Angew. Chem., Int. Ed.* **2013**, *52*, 4012−4015.
(21) Khaskin, E.; Milstein, D. *ACS Catal.* **2013**, *3*, 448−452.
(22) Zhang, L.; Peng, D.; Leng, X.; Huang, Z. *Angew. Chem., Int. Ed.* **2013**, *52*, 3676−3680.
(23) Evans, D. F. *J. Chem. Soc.* **1959**, 2003−2005.
(24) (a) Zhang, J.; Gandelman, M.; Herrman, D.; Leitus, G.; Shimon, L. J. W.; Ben-David, Y.; Milstein, D. *Inorg. Chim. Acta* **2006**, *359*, 1955−1960. (b) Schmiege, B. M.; Carney, M. J.; Small, B. L.; Gerlach, D. L.; Halfen, J. A. *Dalton Trans.* **2007**, 2547−2562.
(25) For selected examples see: (a) de Bruin, B.; Bill, E.; Bothe, E.; Weyhermüller, T.; Wieghardt, K. *Inorg. Chem.* **2000**, *39*, 2936−2947. (b) Danopoulos, A. A.; Tsoureas, N.; Wright, J. A.; Light, M. E. *Organometallics* **2004**, *23*, 166−168. (c) McGuinness, D. S.; Gibson, V. C.; Steed, J. W. *Organometallics* **2004**, *23*, 6288−6292. (d) Benito-Garagorri, D.; Becker, E.; Wiedermann, J.; Lackner, W.; Pollak, M.; Mereiter, K.; Kisala, J.; Kirchner, K. *Organometallics* **2006**, *25*, 1900−1913. (e) Mikhailine, A. A.; Kim, E.; Dingels, C.; Lough, A. J.; Morris, R. H. *Inorg. Chem.* **2008**, *47*, 6587−6589. (f) Chang, M.; Kobayashi, A.; Nakajima, K.; Chang, H.-C.; Kato, M. *Inorg. Chem.* **2011**, *50*, 8308−8317. (g) Craig, G. A.; Costa, J. S.; Roubeau, O.; Teat, S. J.; Aromí, G. *Chem.—Eur. J.* **2012**, *18*, 11703−11715. (h) Šalitroš, I.; Fuhr, O.; Kruk, R.; Pavlik, J.; Pogány, L.; Schäfer, B.; Tatarko, M.; Boča, R.; Linert, W.; Ruben, M. *Eur. J. Inorg. Chem.* **2013**, *2013*, 1049−1057. (i) Harzmann, G. D.; Neuburger, M.; Mayor, M. *Eur. J. Inorg. Chem.* **2013**, *2013*, 3334−3347.
(26) Swart, M. *J. Chem. Theory Comput.* **2008**, *4*, 2057−2066.
(27) Scarborough, C. C.; Wieghardt, K. *Inorg. Chem.* **2011**, *50*, 9773−9793.
(28) (a) Ben-Ari, E.; Leitus, G.; Shimon, L. J. W.; Milstein, D. *J. Am. Chem. Soc.* **2006**, *128*, 15390−15391. (b) Zhang, J.; Leitus, G.; Ben-David, Y.; Milstein, D. *Angew. Chem., Int. Ed.* **2006**, *45*, 1113−1115. (c) Feller, M.; Ben-Ari, E.; Iron, M. A.; Diskin-Posner, Y.; Leitus, G.; Shimon, L. J.; Konstantinovski, L.; Milstein, D. *Inorg. Chem.* **2010**, *49*, 1615−25. (d) Schwartsburd, L.; Iron, M. A.; Konstantinovski, L.; Diskin-Posner, Y.; Leitus, G.; Shimon, L. J. W.; Milstein, D. *Organometallics* **2010**, *29*, 3817−3827. (e) Vogt, M.; Rivada-Wheelaghan, O.; Iron, M. A.; Leitus, G.; Diskin-Posner, Y.; Shimon, L. J. W.; Ben-David, Y.; Milstein, D. *Organometallics* **2013**, *32*, 300−308.
(29) (a) Milstein, D. *Top. Catal.* **2010**, *53*, 915−923. (b) Gunanathan, C.; Milstein, D. *Acc. Chem. Res.* **2011**, *44*, 588−602. (c) Gunanathan, C.; Milstein, D. *Science* **2013**, *341*, 1229712. DOI: 10.1126/science.1229712.
(30) Norrby, T.; Börje, A.; Zhang, L.; Åkermark, B. *Acta Chem. Scand.* **1998**, *52*, 77−85.
(31) Frisch, M. J.; Trucks, G. W.; Schlegel, H. B.; Scuseria, G. E.; Robb, M. A.; Cheeseman, J. R.; Scalmani, G.; Barone, V.; Mennucci, B.; Petersson, G. A.; Nakatsuji, H.; Caricato, M.; Li, X.; Hratchian, H. P.; Izmaylov, A. F.; Bloino, J.; Zheng, G.; Sonnenberg, J. L.; Hada, M.; Ehara, M.; Toyota, K.; Fukuda, R.; Hasegawa, J.; Ishida, M.; Nakajima, T.; Honda, Y.; Kitao, O.; Nakai, H.; Vreven, T.; Montgomery, J. A.; , Jr., Peralta, J. E.; Ogliaro, F.; Bearpark, M.; Heyd, J. J.; Brothers, E.; Kudin, K. N.; Staroverov, V. N.; Kobayashi, R.; Normand, J.; Raghavachari, K.; Rendell, A.; Burant, J. C.; Iyengar, S. S.; Tomasi, J.; Cossi, M.; Rega, N.; Millam, J. M.; Klene, M.; Knox, J. E.; Cross, J. B.; Bakken, V.; Adamo, C.; Jaramillo, J.; Gomperts, R.; Stratmann, R. E.; Yazyev, O.; Austin, A. J.; Cammi, R.; Pomelli, C.; Ochterski, J. W.; Martin, R. L.; Morokuma, K.; Zakrzewski, V. G.; Voth, G. A.; Salvador, P.; Dannenberg, J. J.; Dapprich, S.; Daniels, A. D.; Farkas, O.; Foresman, J. B.; Ortiz, J. V.; Cioslowski, J.; Fox, D. J. *Gaussian 09*, Revision C.01; Gaussian, Inc.: Wallingford, CT, 2009.
(32) (a) Perdew, J. P.; Burke, K.; Ernzerhof, M. *Phys. Rev. Lett.* **1996**, *77*, 3865−3868. (b) Perdew, J. P.; Burke, K.; Ernzerhof, M. *Phys. Rev. Lett.* **1997**, *78*, 1396.
(33) Kozuch, S.; Martin, J. M. L. *Phys. Chem. Chem. Phys.* **2011**, *13*, 20104−20107.
(34) (a) Adamo, C.; Barone, V. *J. Chem. Phys.* **1999**, *110*, 6158−6170. (b) Perdew, J. P.; Burke, K.; Ernzerhof, M. *Phys. Rev. Lett.* **1997**, *78*, 1396−1396. (c) Perdew, J. P.; Burke, K.; Ernzerhof, M. *Phys. Rev. Lett.* **1996**, *77*, 3865−3868.
(35) Perdew, J. P. *Phys. Rev. B* **1986**, *33*, 8822−8824.
(36) (a) Szabados, Å. *J. Chem. Phys.* **2006**, *125*, 214105. (b) Grimme, S. *J. Chem. Phys.* **2003**, *118*, 9095−9102.
(37) Møller, C.; Plesset, M. S. *Phys. Rev.* **1934**, *46*, 618−622.
(38) (a) Grimme, S.; Antony, J.; Ehrlich, S.; Kreig, H. *J. Chem. Phys.* **2010**, *132*, 154104. (b) Schwabe, T.; Grimme, S. *Acc. Chem. Res.* **2008**, *41*, 569−579. (c) Schwabe, T.; Grimme, S. *Phys. Chem. Chem. Phys.* **2007**, *9*, 3397−3406. (d) Grimme, S. *J. Comput. Chem.* **2006**, *27*, 1787−1799.
(39) Grimme, S.; Ehrlich, S.; Goerigk, L. *J. Comput. Chem.* **2011**, *32*, 1456−1465.
(40) (a) Johnson, E. R.; Becke, A. D. *J. Chem. Phys.* **2006**, *124*, 174104. (b) Johnson, E. R.; Becke, A. D. *J. Chem. Phys.* **2005**, *123*, 024101.
(41) (a) Schäfer, A.; Horn, H.; Ahlrichs, R. *J. Chem. Phys.* **1992**, *97*, 2571−2577. (b) Schäfer, A.; Huber, C.; Ahlrichs, R. *J. Chem. Phys.* **1994**, *100*, 5829−5835.
(42) (a) Dunlap, B. I. *J. Chem. Phys.* **1983**, *78*, 3140−3142. (b) Dunlap, B. I. *J. Mol. Struct. (THEOCHEM)* **2000**, *529*, 37−40.
(43) (a) Eichkorn, K.; Treutler, O.; Öhm, H.; Häser, M.; Ahlrichs, R. *Chem. Phys. Lett.* **1995**, *240*, 283−290. (b) Eichkorn, K.; Weigend, F.; Treutler, O.; Ahlrichs, R. *Theor. Chem. Acc.* **1997**, *97*, 119−124.
(44) (a) Schwabe, T.; Grimme, S. *Phys. Chem. Chem. Phys.* **2007**, *9*, 3397−3406. (b) Schwabe, T.; Grimme, S. *Acc. Chem. Res.* **2008**, *41*, 569−579.
(45) (a) Mennucci, B.; Tomasi, J. *J. Chem. Phys.* **1997**, *106*, 5151−5158. (b) Cancès, E.; Mennucci, B.; Tomasi, J. *J. Chem. Phys.* **1997**, *107*, 3032−3041. (c) Cossi, M.; Barone, V.; Mennucci, B.; Tomasi, J. *Chem. Phys. Lett.* **1998**, *286*, 253−260. (d) Cossi, M.; Scalmani, G.; Rega, N.; Barone, V. *J. Chem. Phys.* **2002**, *117*, 43−54.
(46) (a) Mennucci, B.; Cancès, E.; Tomasi, J. *J. Phys. Chem. B* **1997**, *101*, 10506−10517. (b) Tomasi, J.; Mennucci, B.; Cancès, E. *J. Mol. Struct. (THEOCHEM)* **1999**, *464*, 211−226.

(47) Marenich, A. V.; Cramer, C. J.; Truhlar, D. G. *J. Phys. Chem. B* **2009**, *113*, 6378−6396.
(48) (a) Hegarty, D.; Robb, M. A. *Mol. Phys.* **1979**, *38*, 1795−1812. (b) Eade, R. H. A.; Robb, M. A. *Chem. Phys. Lett.* **1981**, *83*, 362−368. (c) Schlegel, H. B.; Robb, M. A. *Chem. Phys. Lett.* **1982**, *93*, 43−46. (d) Bernardi, F.; Andrea, B.; McDouall, J. J. W.; Robb, M. A.; Schlegel, H. B. *Faraday Symp. Chem. Soc.* **1984**, *19*, 137−147. (e) Frisch, M. J.; Ragazos, I. N.; Robb, M. A.; Schlegel, H. B. *Chem. Phys. Lett.* **1992**, *189*, 524−528. (f) Yamamoto, N.; Vreven, T.; Robb, M. A.; Frisch, M. J.; Schlegel, H. B. *Chem. Phys. Lett.* **1996**, *250*, 373−378. (g) Schmidt, M. W.; Gordon, M. S. *Annu. Rev. Phys. Chem.* **1998**, *49*, 233−266.
(49) (a) Angeli, C.; Cimiraglia, R.; Evangelisti, S.; Leininger, T.; Malrieu, J.-P. *J. Chem. Phys.* **2001**, *114*, 10252−10264. (b) Angeli, C.; Cimiraglia, R.; Malrieu, J.-P. *Chem. Phys. Lett.* **2001**, *350*, 297−305. (c) Angeli, C.; Cimiraglia, R.; Malrieu, J.-P. *J. Chem. Phys.* **2002**, *117*, 9138−9153.
(50) Neese, F.; Wennmohs, F. *Orca, an ab initio, DFT and semiempirical SCF-MO package*, Version 2.9.0; with contributions from Becker, U.; Bykov, D.; Ganyushin, D.; Hansen, A.; Izsak, R.; Liakos, D. G.; Kollmar, C.; Kossmann, S.; Pantazis, D. A.; Petrenko, T.; Reimann, C.; Riplinger, C.; Roemelt, M.; Sandhöfer, B.; Schapiro, I.; Sivalingam, K.; Wezisla, B.; Kállay, M.; Grimme, S.; Valeev, E.; Max Planck Institute for Bioinorganic Chemistry: Mülheim an der Ruhr, Germany, 2012.
(51) (a) Neese, F. *J. Comput. Chem.* **2003**, *24*, 1740−1747. (b) Neese, F.; Wennmohs, F.; Hansen, A.; Becker, U. *Chem. Phys.* **2009**, *356*, 98−109. (c) Kossmann, S.; Neese, F. *Chem. Phys. Lett.* **2009**, *481*, 240−243. (d) Kossmann, S.; Neese, F. *J. Chem. Theory Comput.* **2010**, *6*, 2325−2338. (e) Izsák, R.; Neese, F. *J. Chem. Phys.* **2011**, *135*, 144105.